Supporting Information

Synthesis and characterization of Pd/NHC$_F$ complexes with fluorinated aryl groups

Darya O. Prima[§], Roman O. Pankov[§], Alexander Yu. Kostyukovich,[§] Mikhail E. Minyaev[§], Julia V. Burykina[§], Valentine P. Ananikov[§*]

[§] *Zelinsky Institute of Organic Chemistry, Russian Academy of Sciences, Leninsky prospekt 47, Moscow, 119991, Russia;*

**e-mail: val@ioc.ac.ru; http://AnanikovLab.ru*

Contents

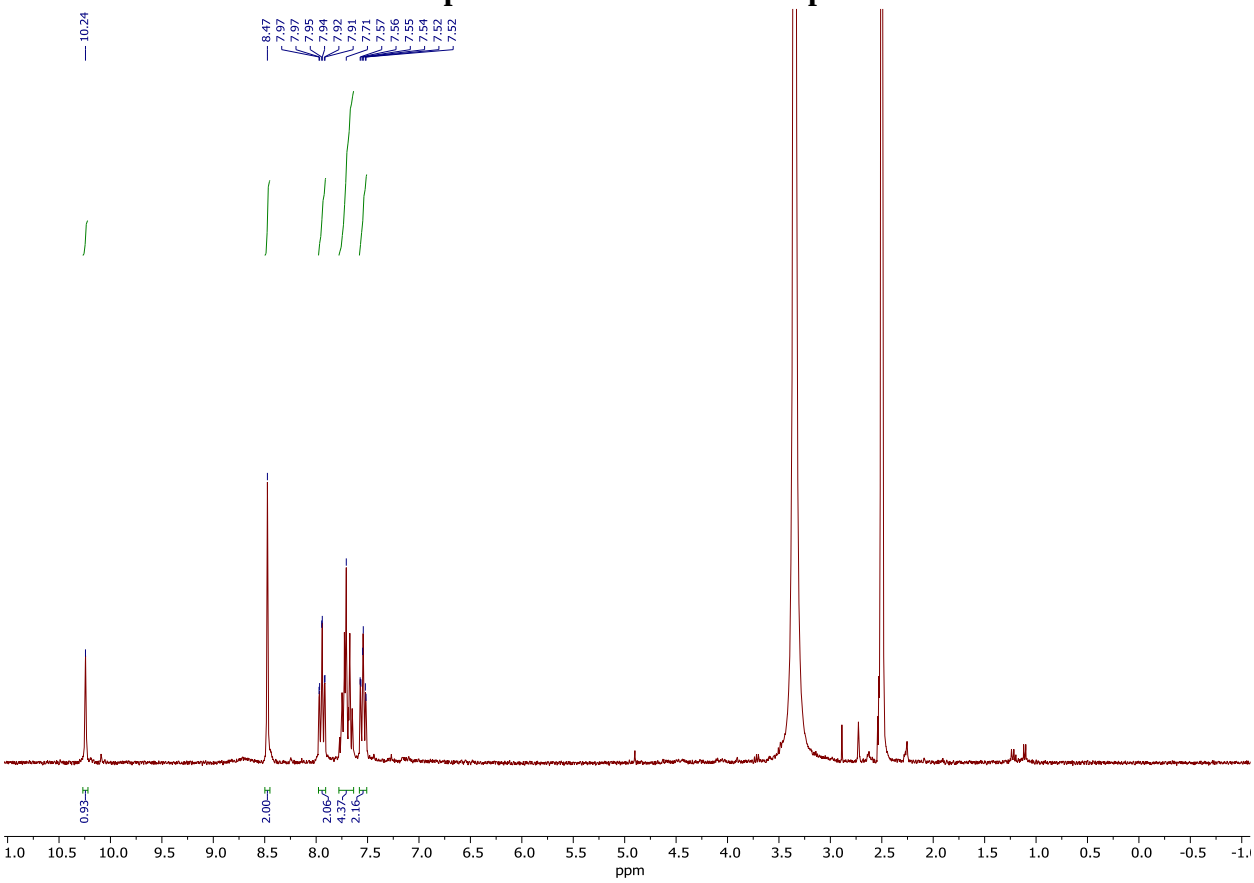

Figure S1. ^{1}H NMR spectrum of **3a**. Solvent: DMSO-d_6, 300 MHz.

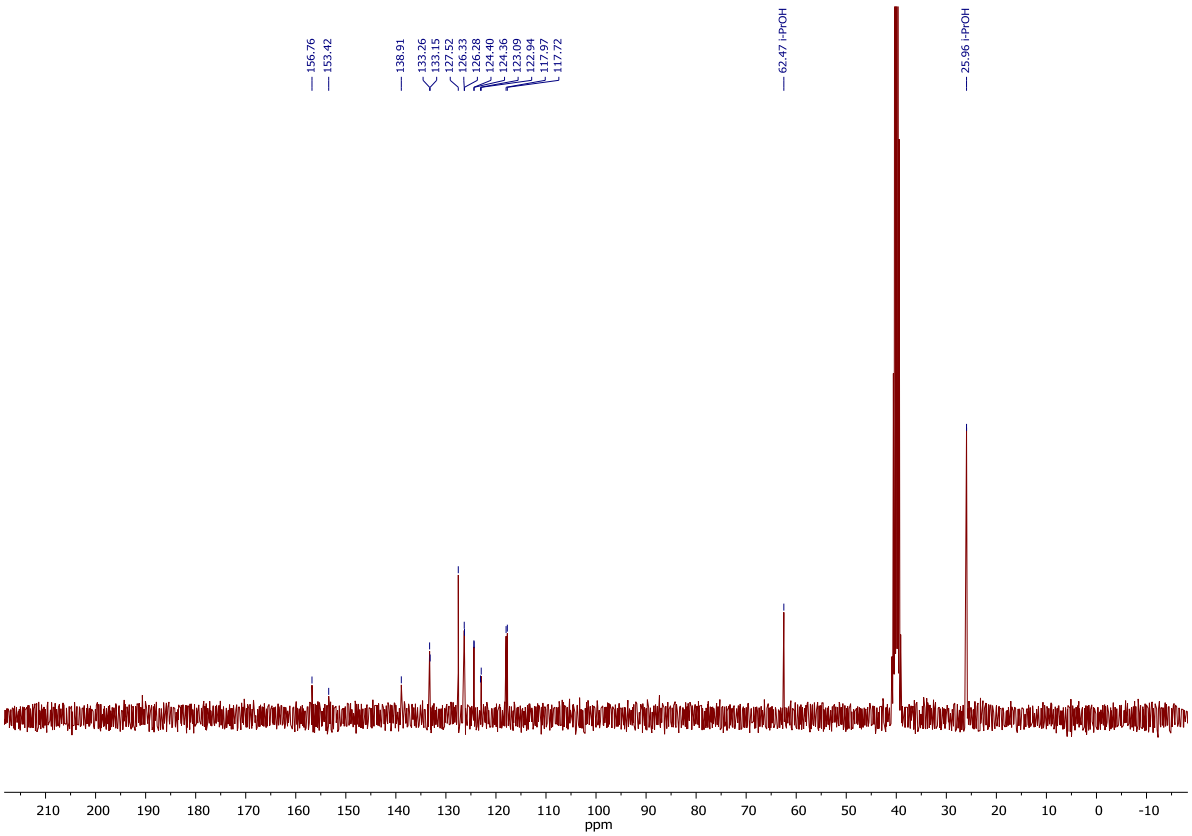

Figure S2. ^{13}C{^{1}H} NMR spectrum of **3a**. Solvent: DMSO-d_6, 75 MHz.

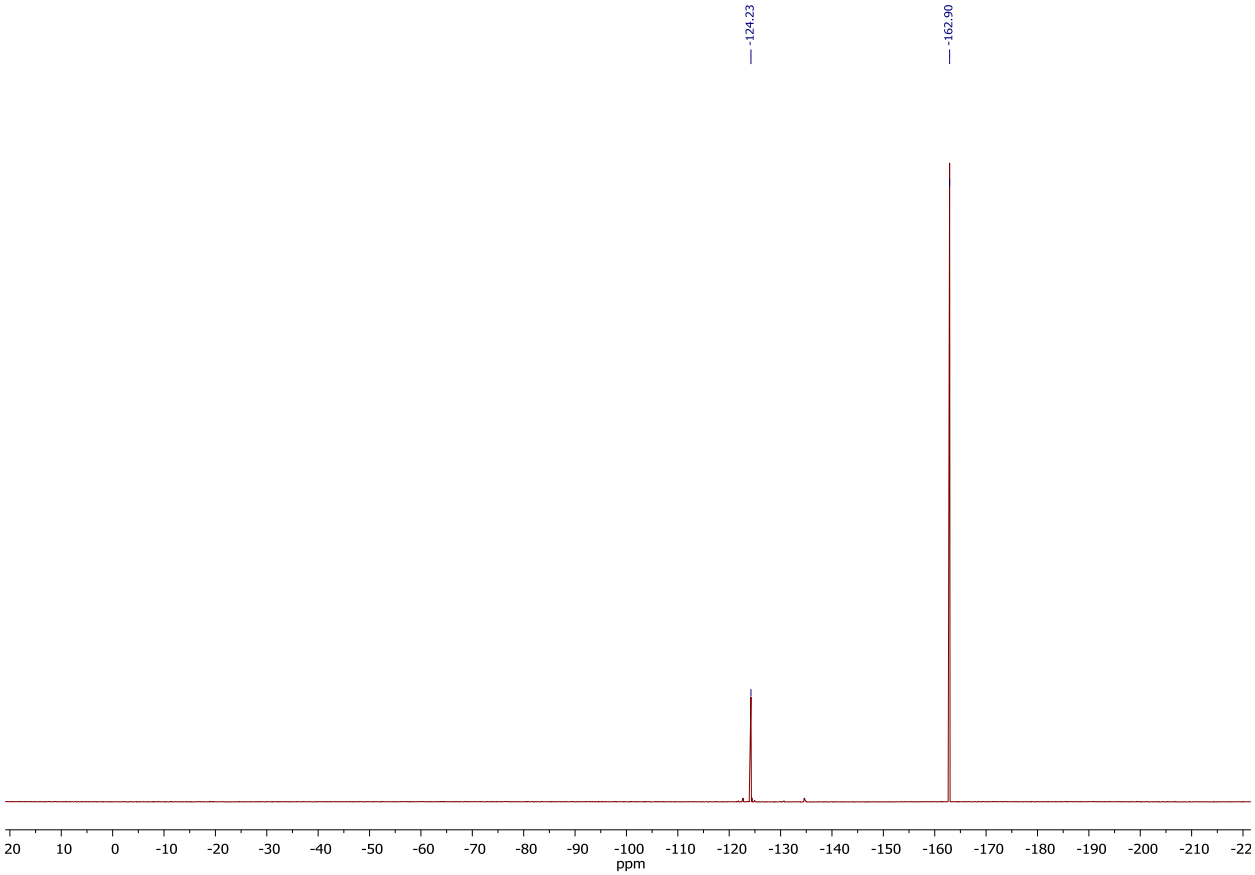

Figure S3. $^{19}F\{^{1}H\}$ NMR spectrum of **3a**. Solvent: DMSO-d_6, 282.4 MHz. Standard: C_6F_6 with respect to $CFCl_3$.

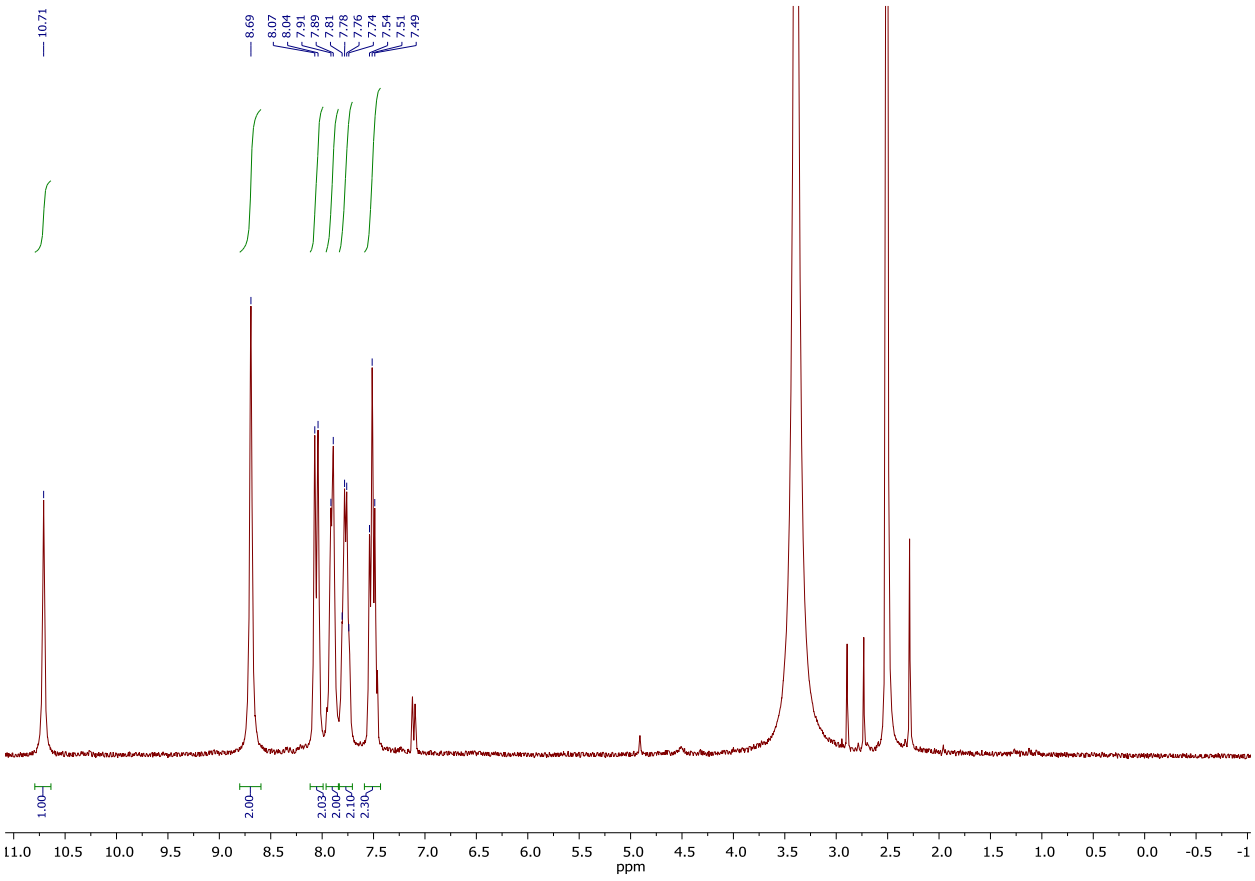

Figure S4. ^{1}H NMR spectrum of **3b**. Solvent: DMSO-d_6, 300 MHz.

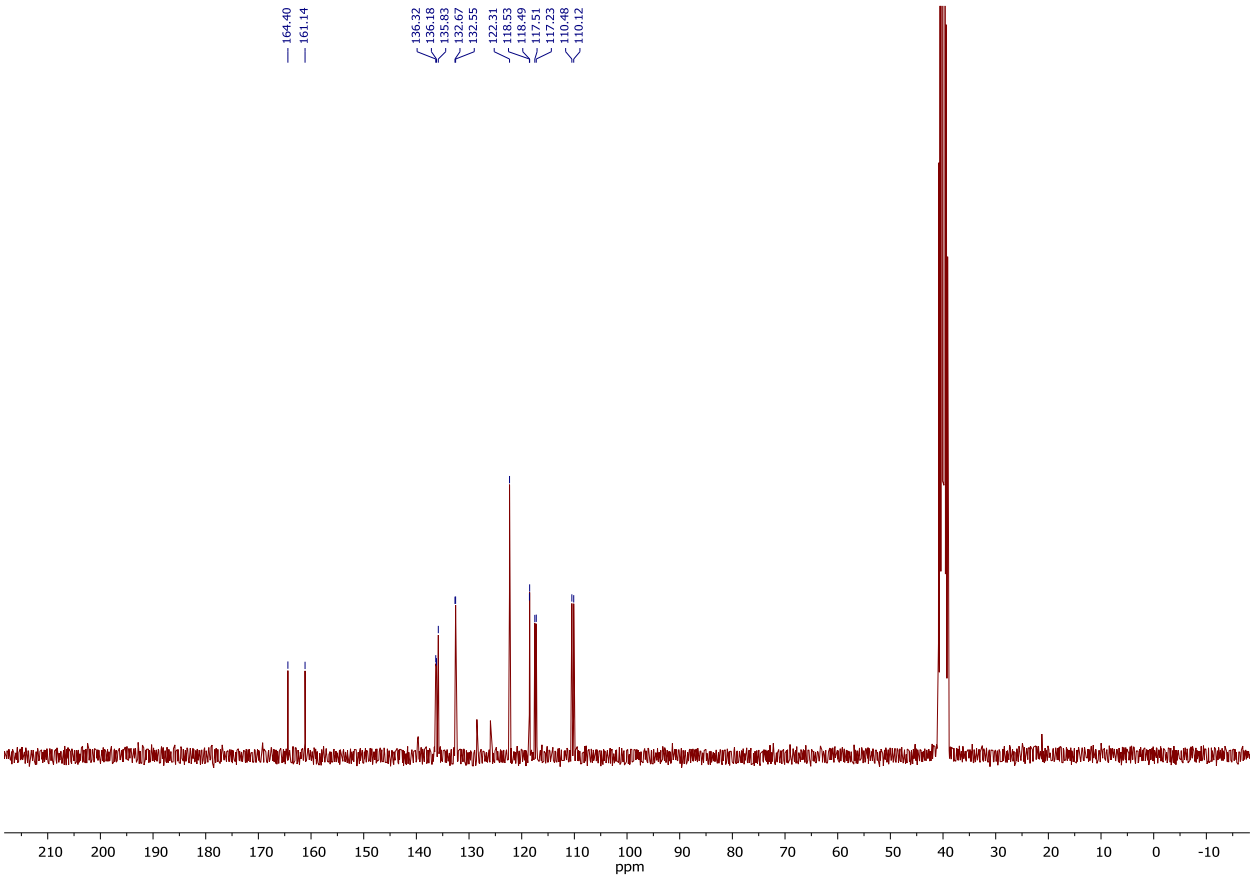

Figure S5. $^{13}C\{^{1}H\}$ NMR spectrum of **3b**. Solvent: DMSO-d_6, 75 MHz.

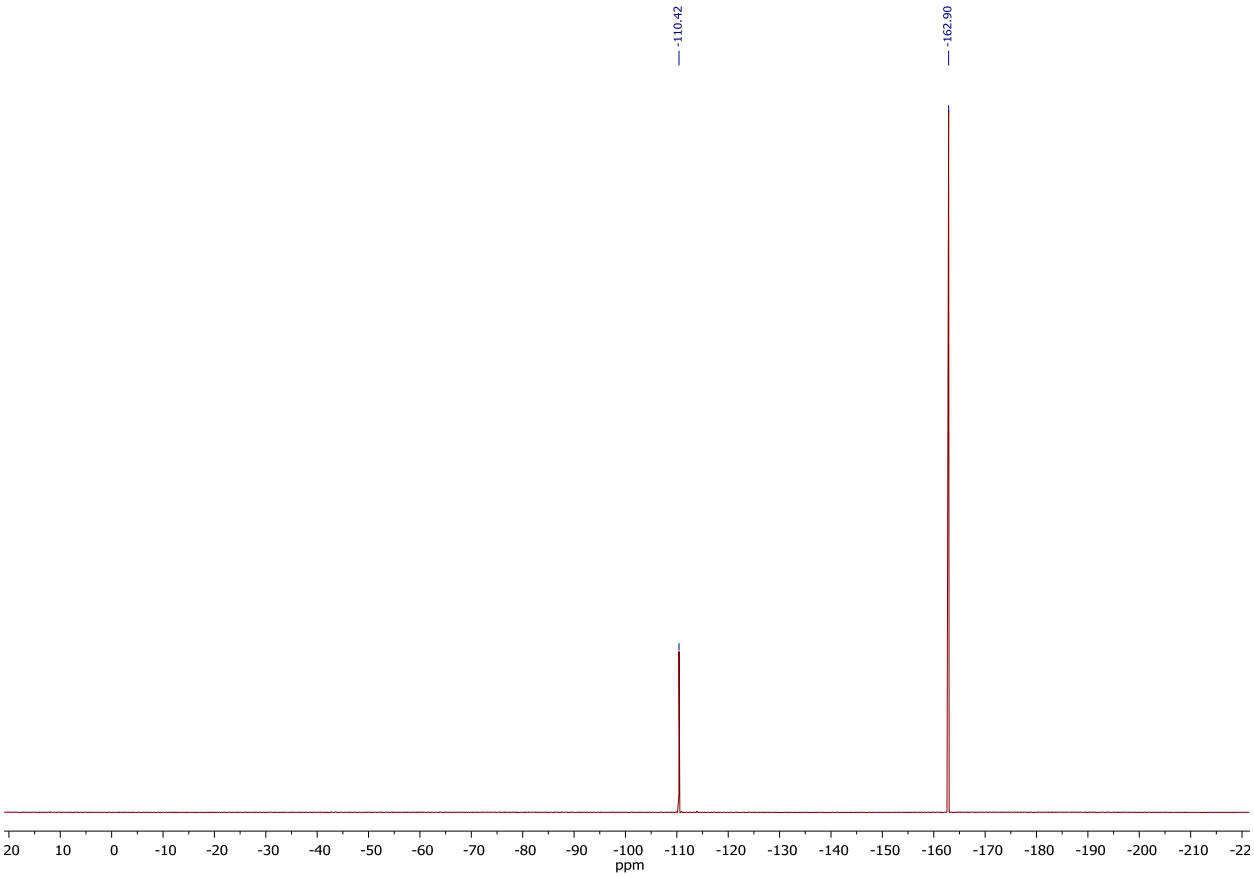

Figure S6. $^{19}F\{^{1}H\}$ NMR spectrum of **3b**. Solvent: DMSO-d_6, 282.4 MHz. Standard: C_6F_6 with respect to $CFCl_3$.

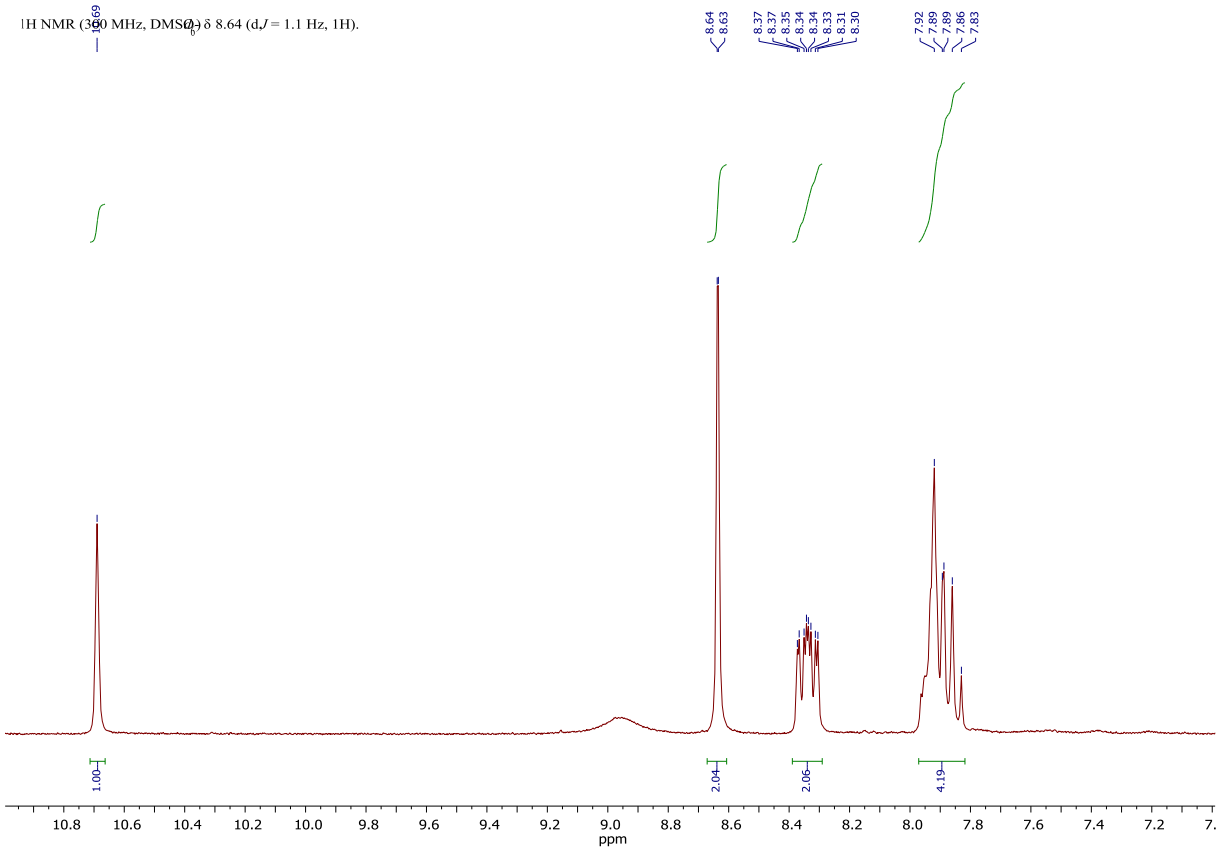

Figure S7. ^{1}H NMR spectrum of **3c**. Solvent: DMSO-d_6, 300 MHz.

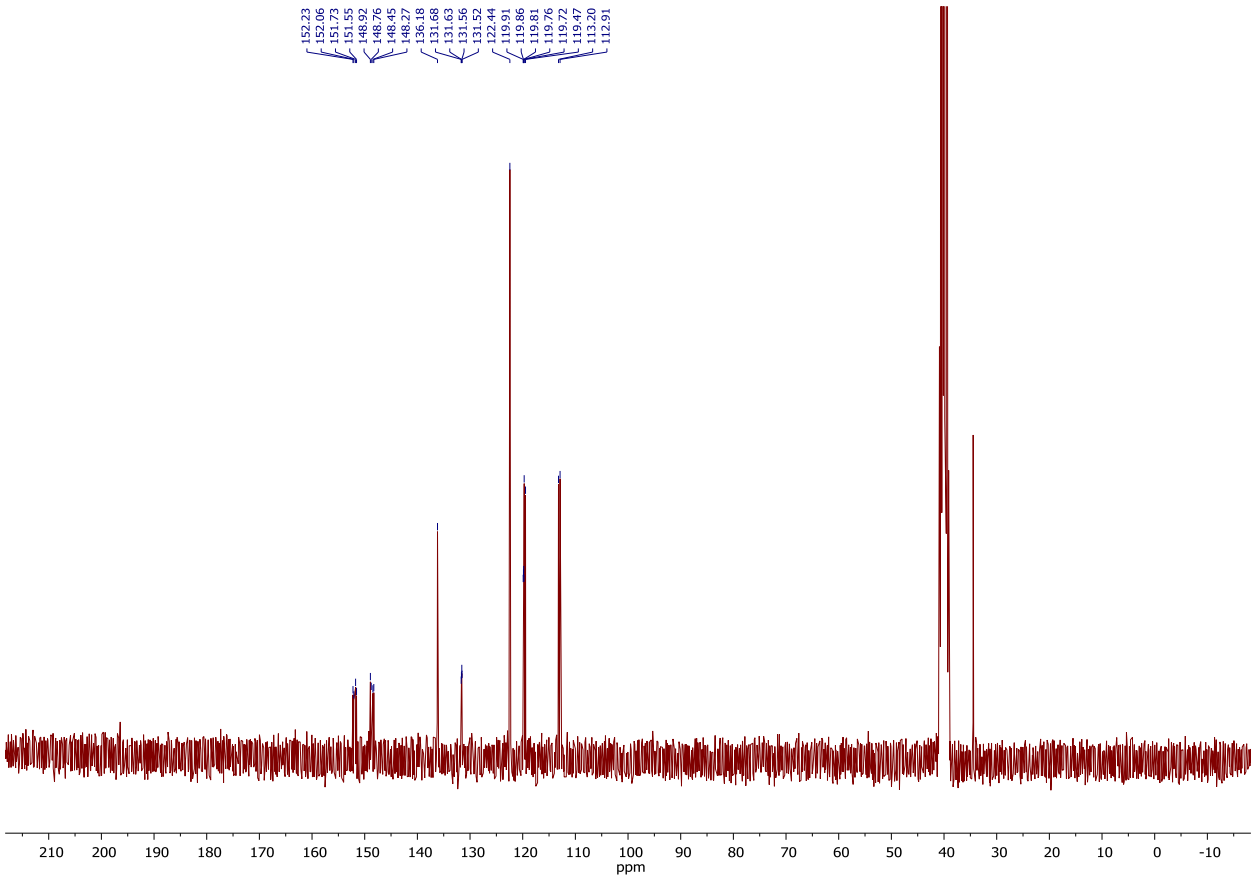

Figure S8. ^{13}C{^{1}H} NMR spectrum of **3c**. Solvent: DMSO-d_6, 75 MHz.

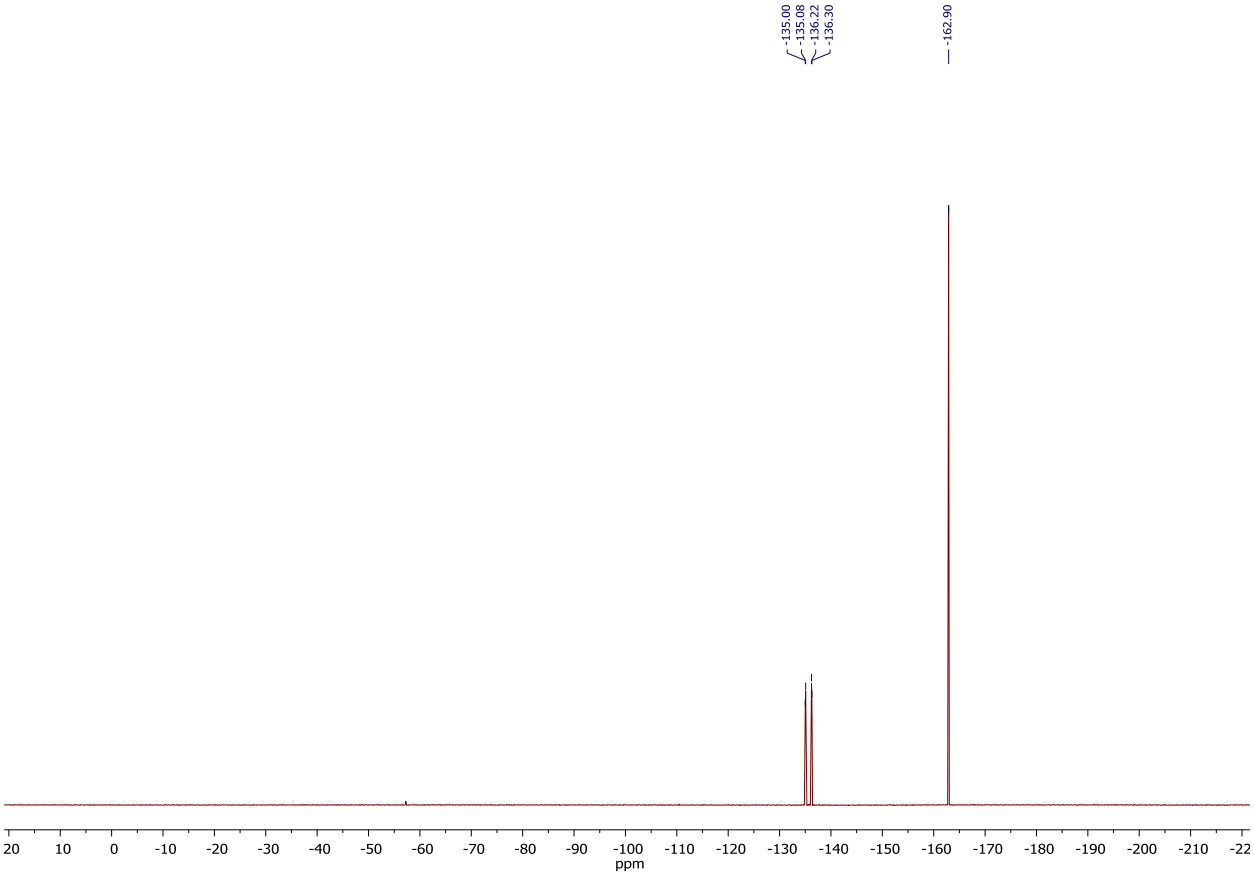

Figure S9. $^{19}F\{^{1}H\}$ NMR spectrum of **3c**. Solvent: DMSO-d_6, 282.4 MHz. Standard: C_6F_6 with respect to $CFCl_3$.

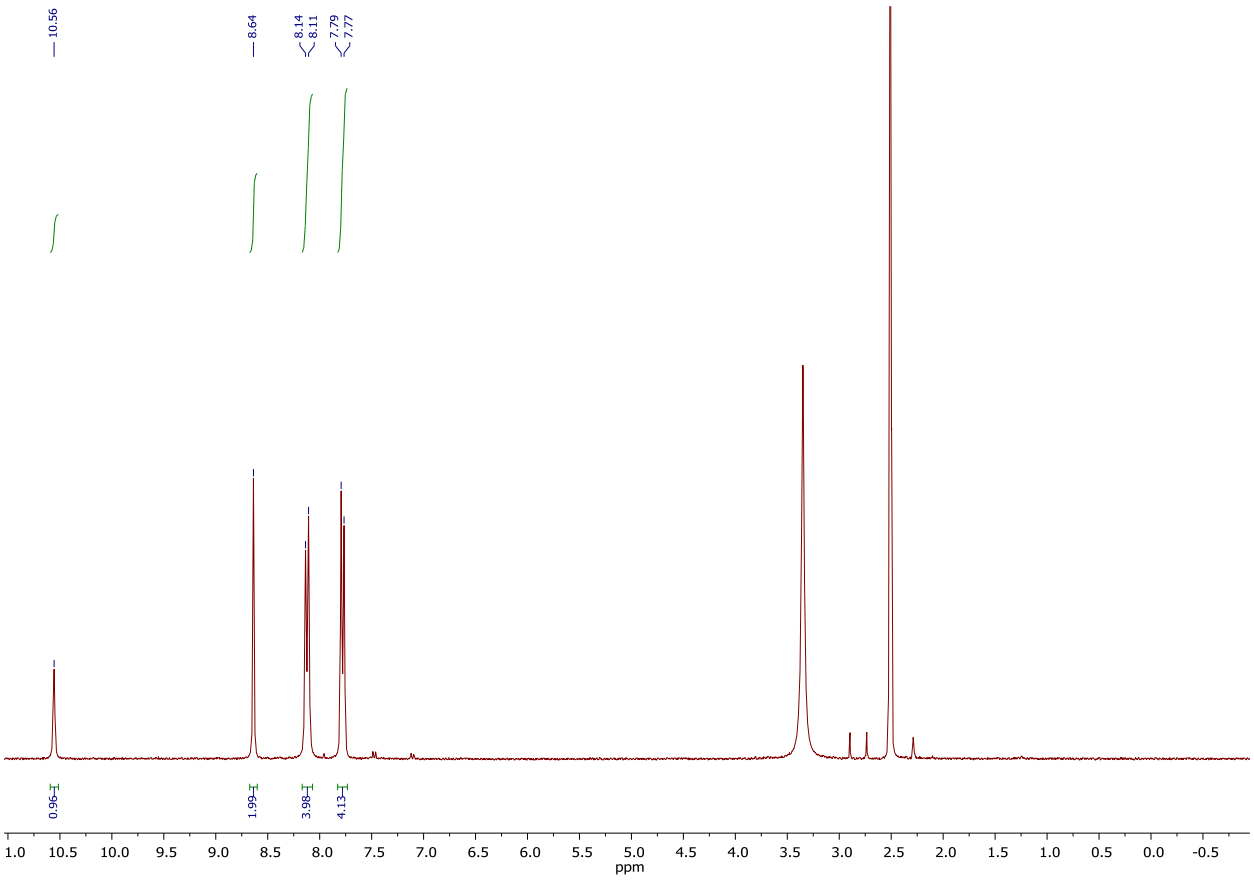

Figure S10. ^{1}H NMR spectrum of **3d**. Solvent: DMSO-d_6, 300 MHz.

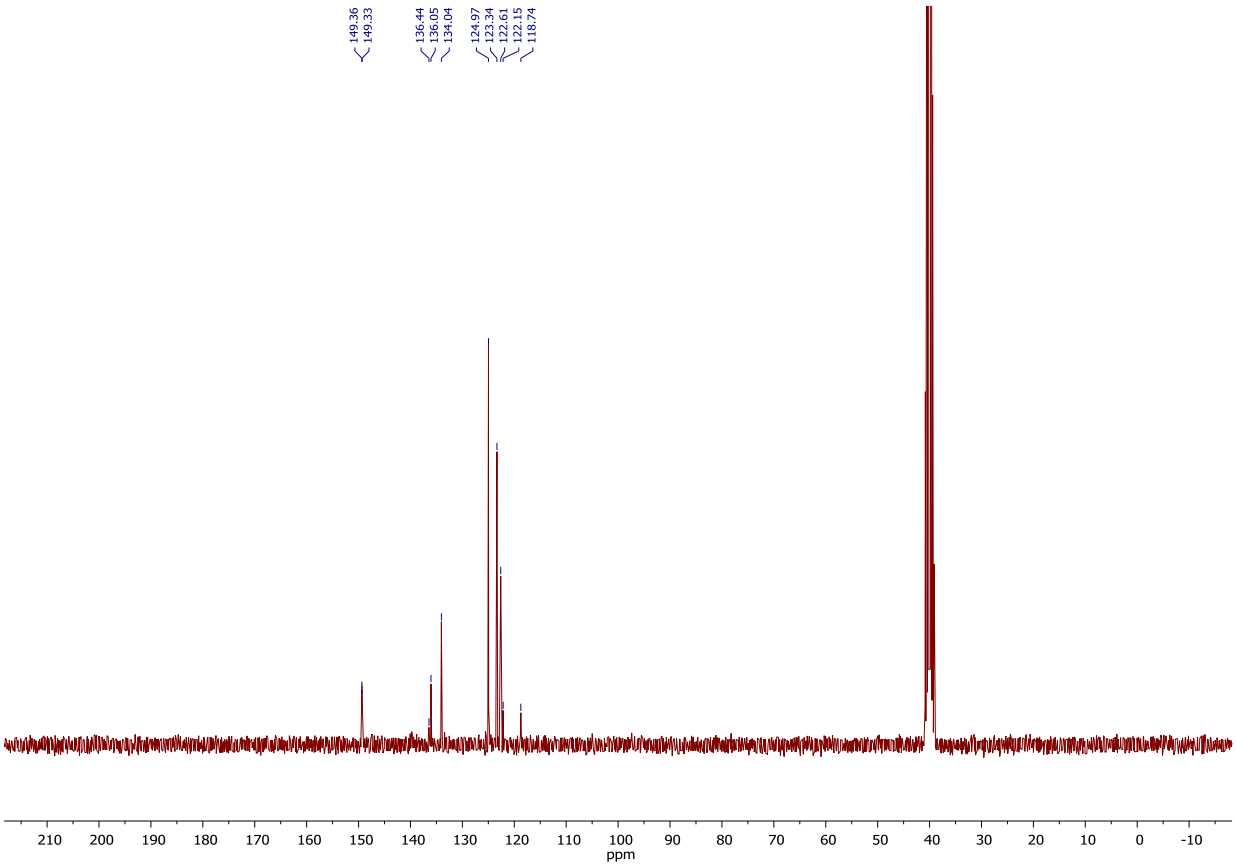

Figure S11. $^{13}C\{^{1}H\}$ NMR spectrum of **3d**. Solvent: DMSO-d_6, 75 MHz.

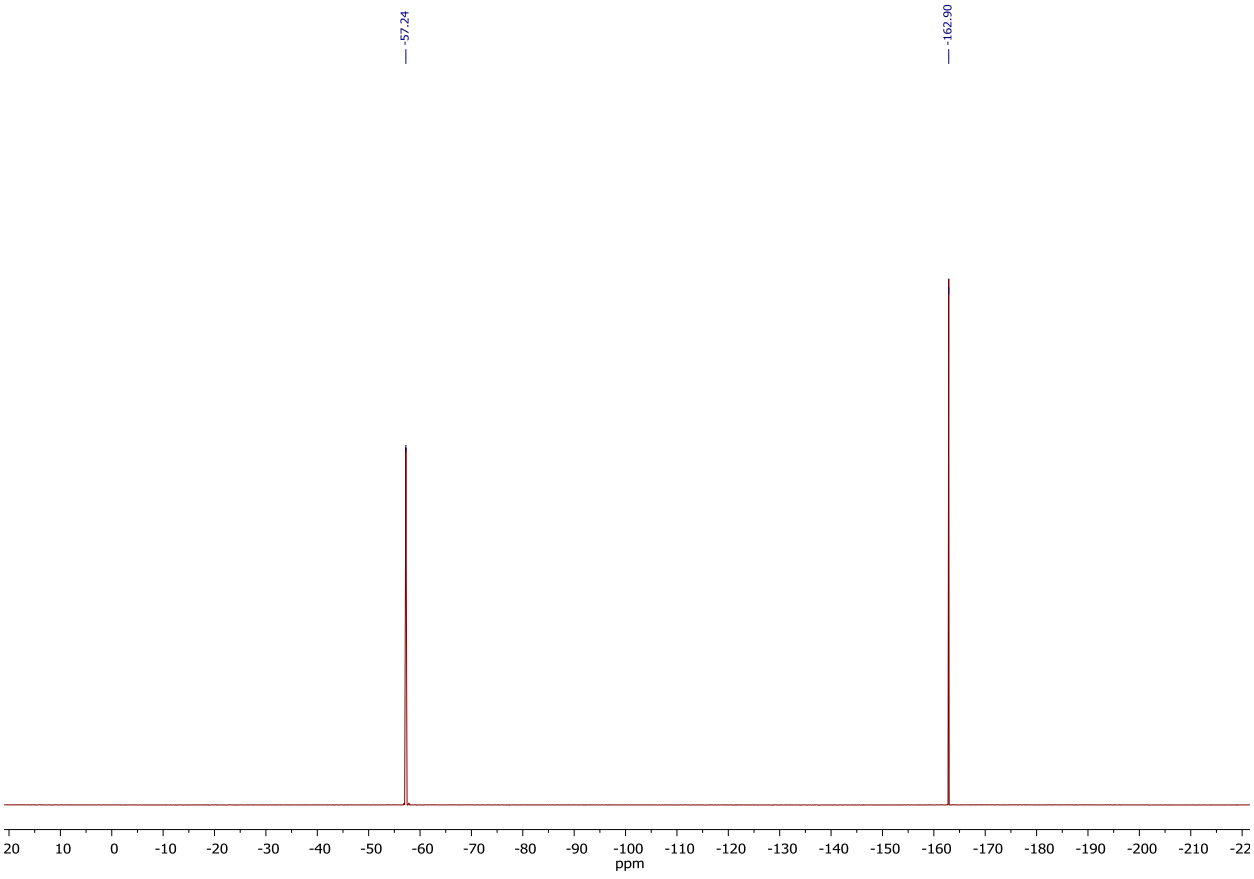

Figure S12. $^{19}F\{^{1}H\}$ NMR spectrum of **3d**. Solvent: DMSO-d_6, 282.4 MHz. Standard: C_6F_6 with respect to $CFCl_3$.

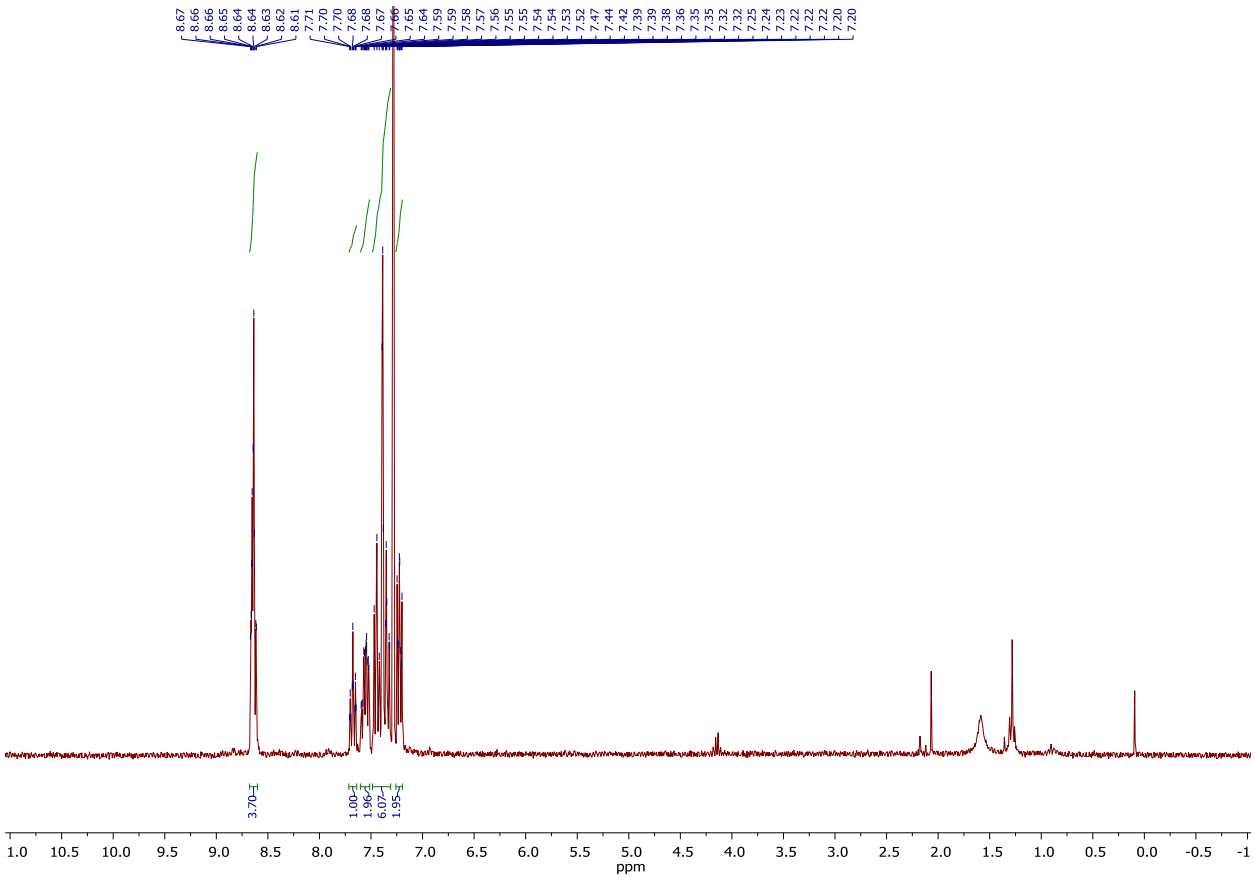

Figure S13. ^{1}H NMR spectrum of **4a**. Solvent: $CDCl_3$, 300 MHz.

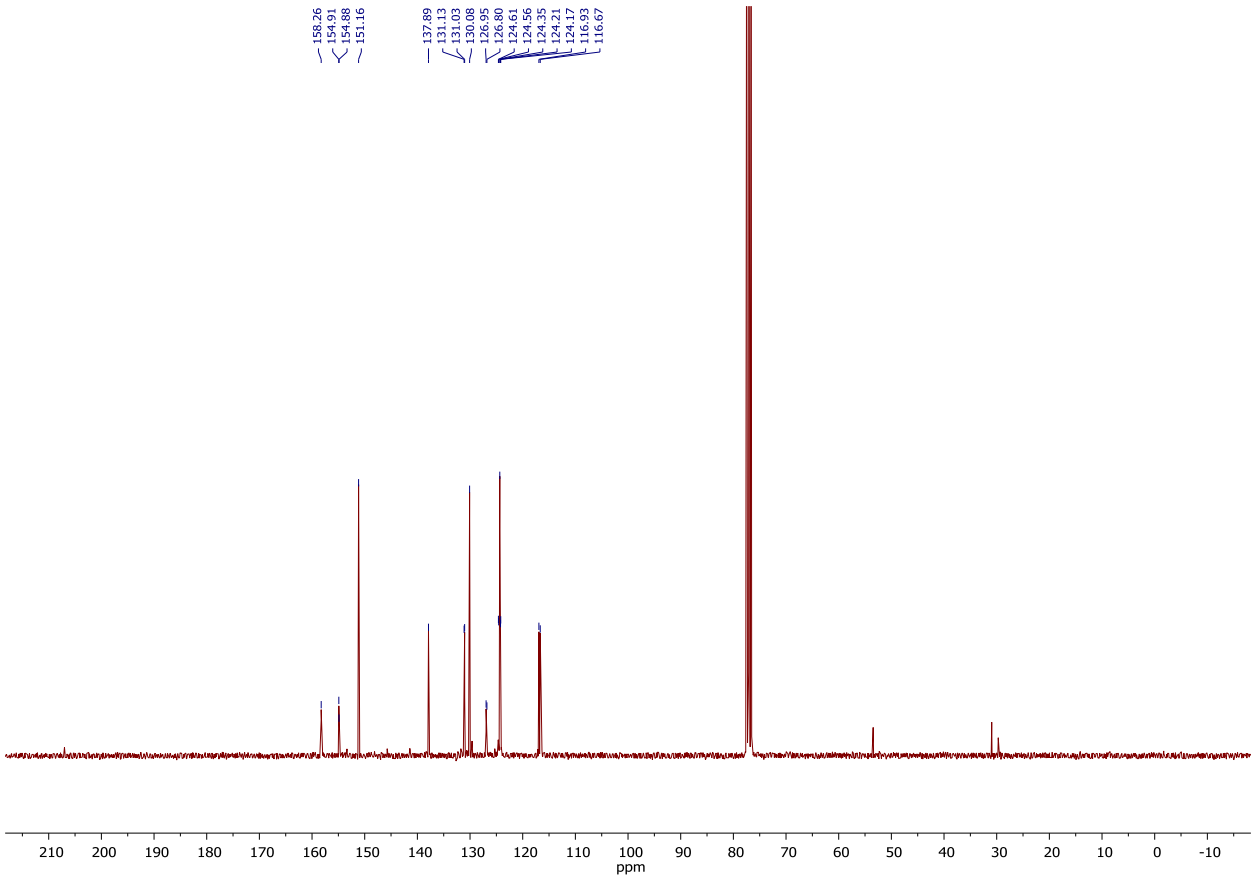

Figure S14. $^{13}C\{^{1}H\}$ NMR spectrum of **4a**. Solvent: $CDCl_3$, 75 MHz.

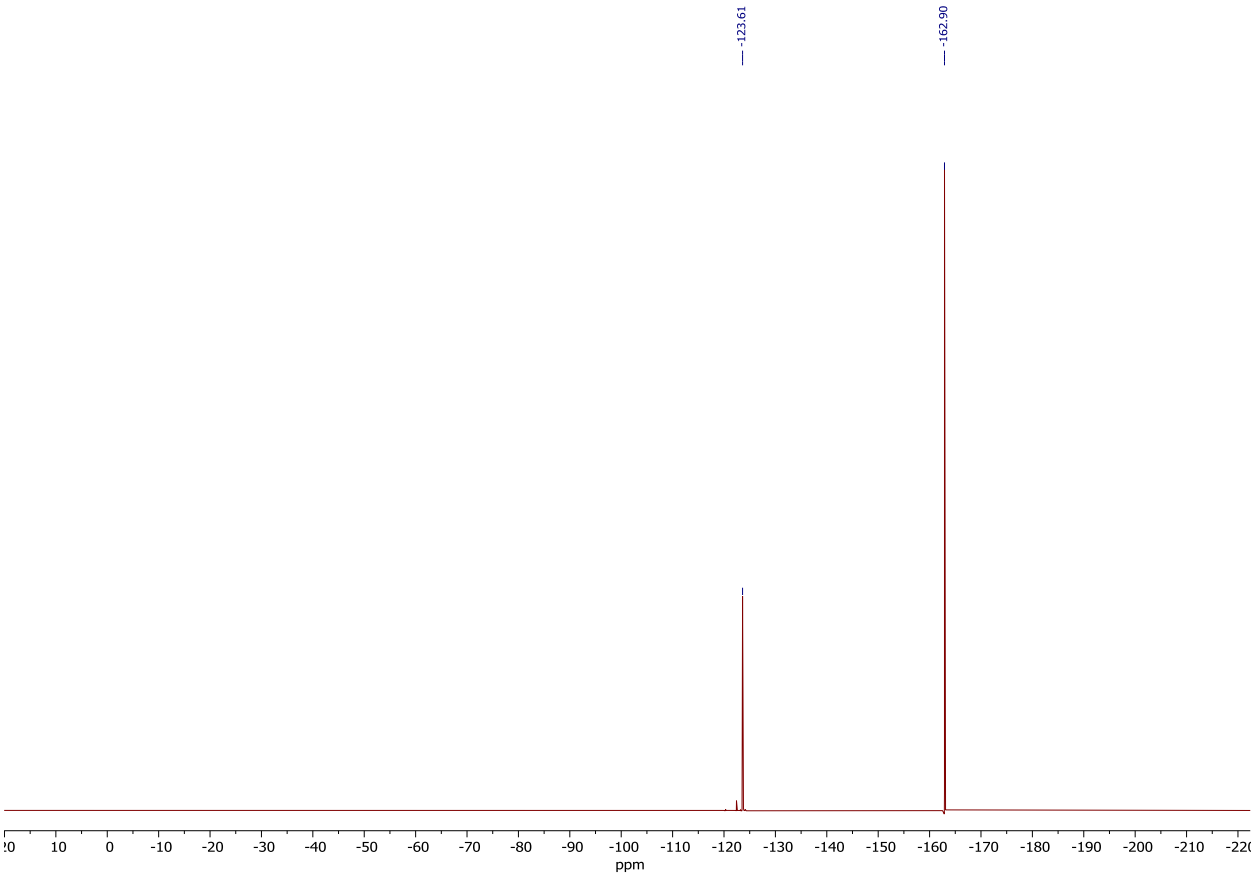

Figure S15. $^{19}F\{^{1}H\}$ NMR spectrum of **4a**. Solvent: $CDCl_3$, 282.4 MHz. Standard: C_6F_6 with respect to $CFCl_3$.

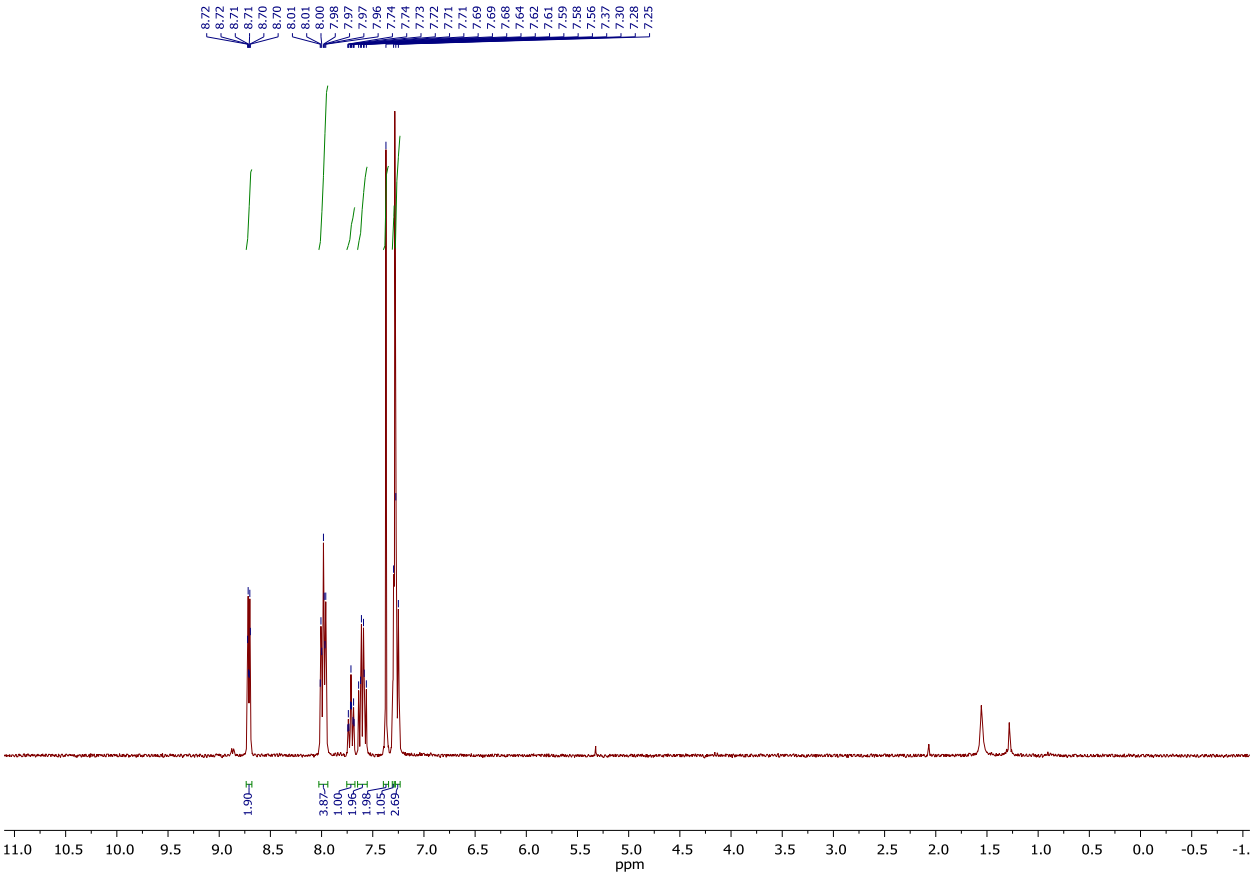

Figure S16. ^{1}H NMR spectrum of **4b**. Solvent: $CDCl_3$, 300 MHz.

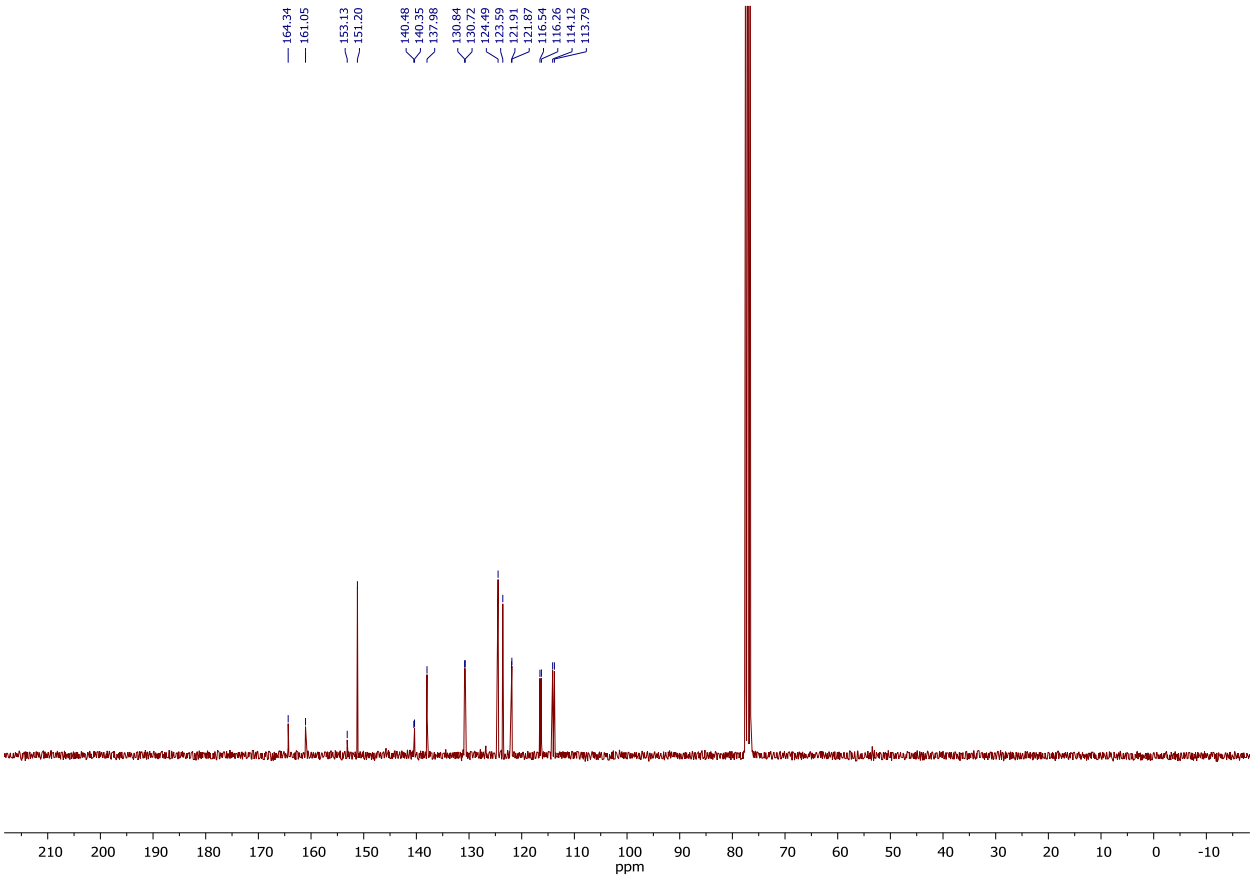

Figure S17. $^{13}C\{^{1}H\}$ NMR spectrum of **4b**. Solvent: $CDCl_3$, 75 MHz.

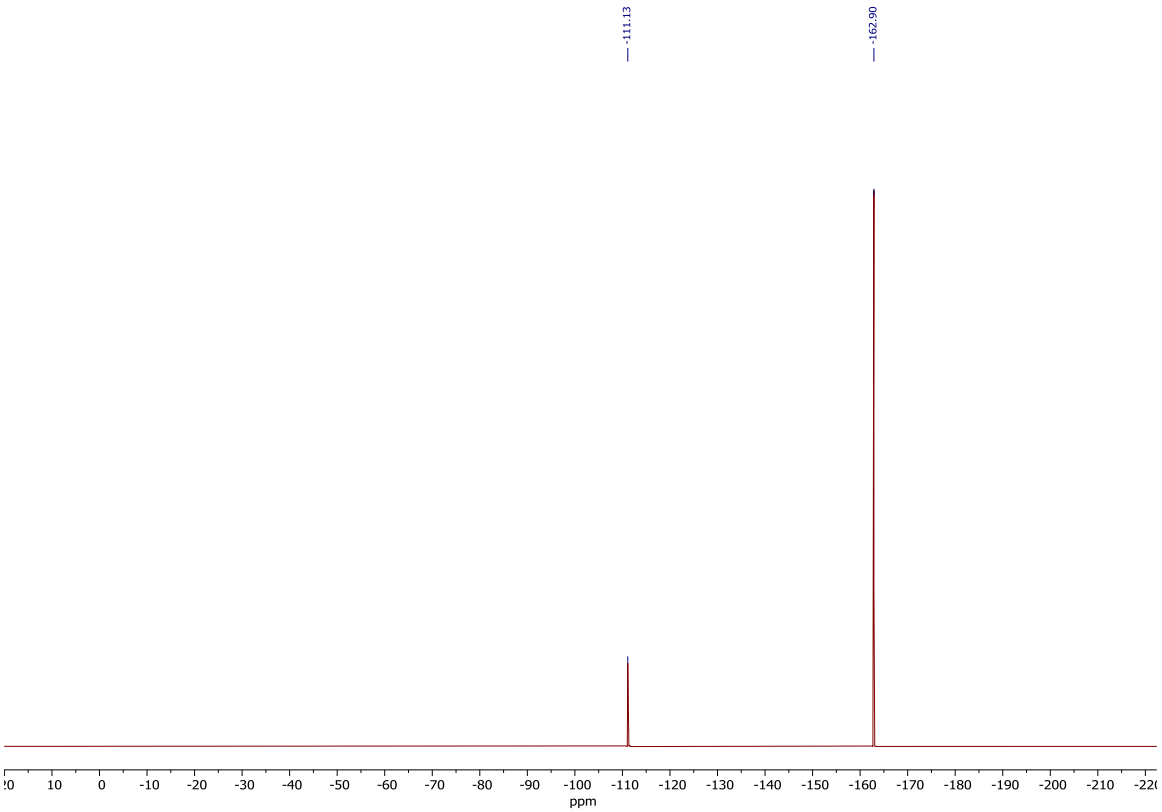

Figure S18. $^{19}F\{^{1}H\}$ NMR spectrum of **4b**. Solvent: $CDCl_3$, 282.4MHz. Standard: C_6F_6 with respect to $CFCl_3$.

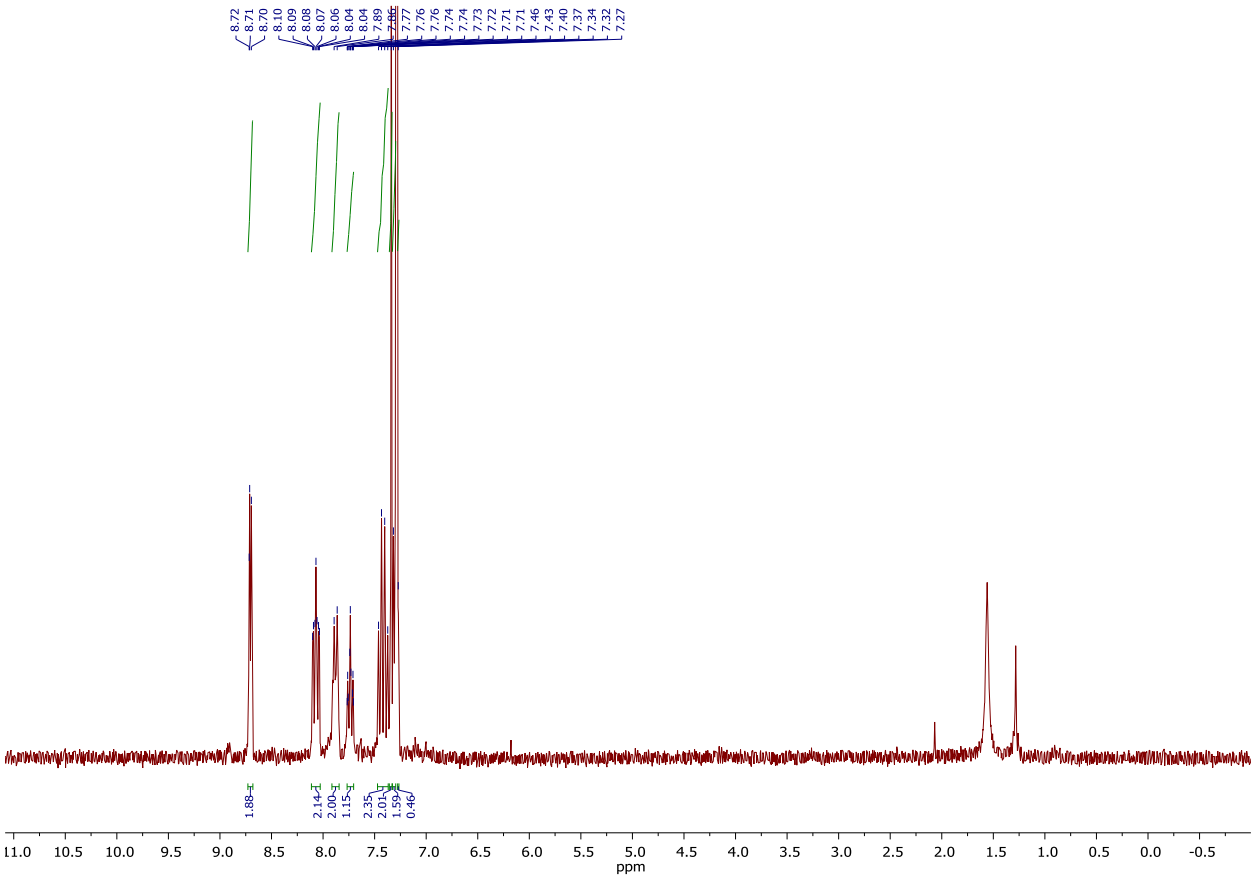

Figure S19. ^{1}H NMR spectrum of **4c**. Solvent: $CDCl_3$, 300 MHz.

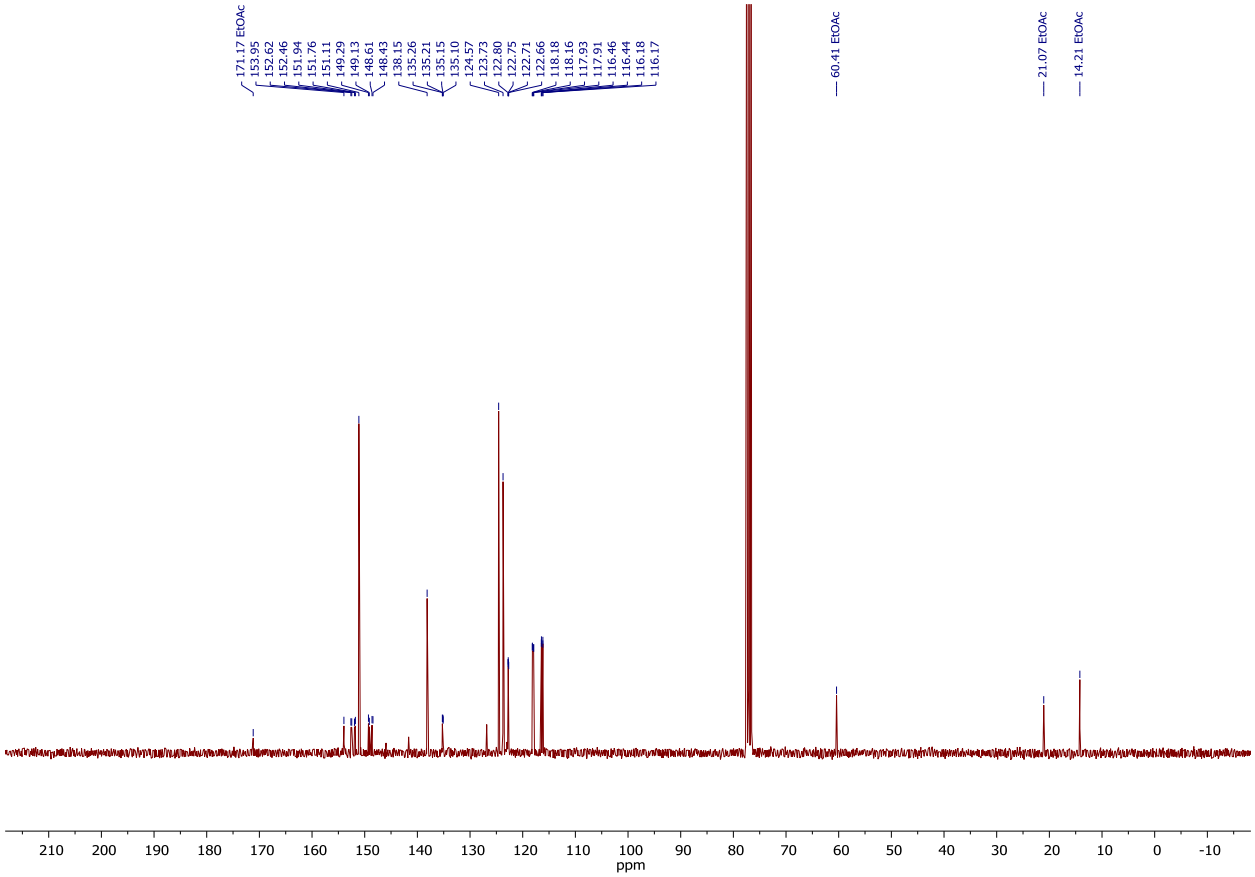

Figure S20. $^{13}C\{^{1}H\}$ NMR spectrum of **4c**. Solvent: $CDCl_3$, 75 MHz.

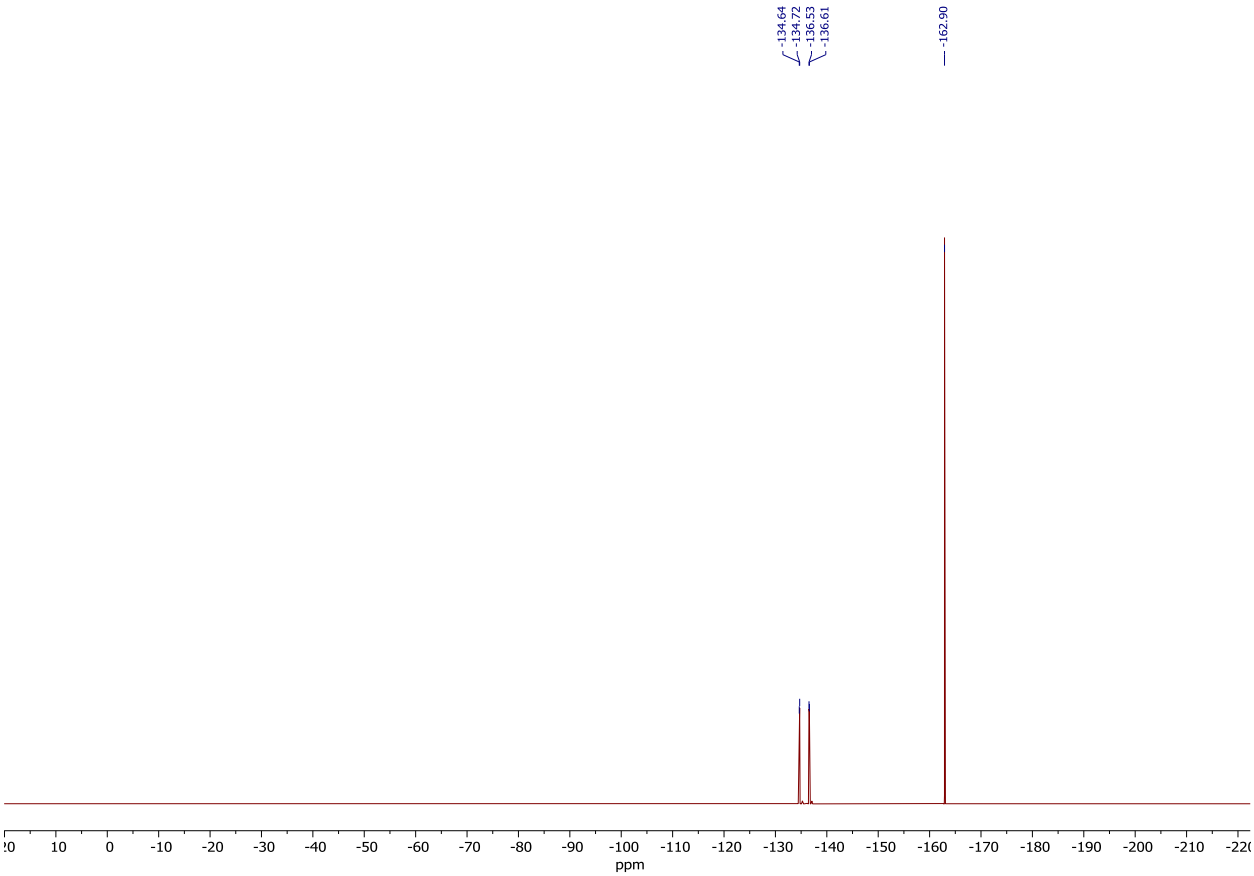

Figure S21. $^{19}F\{^{1}H\}$ NMR spectrum of **4c**. Solvent: $CDCl_3$, 282.4 MHz. Standard: C_6F_6 with respect to $CFCl_3$.

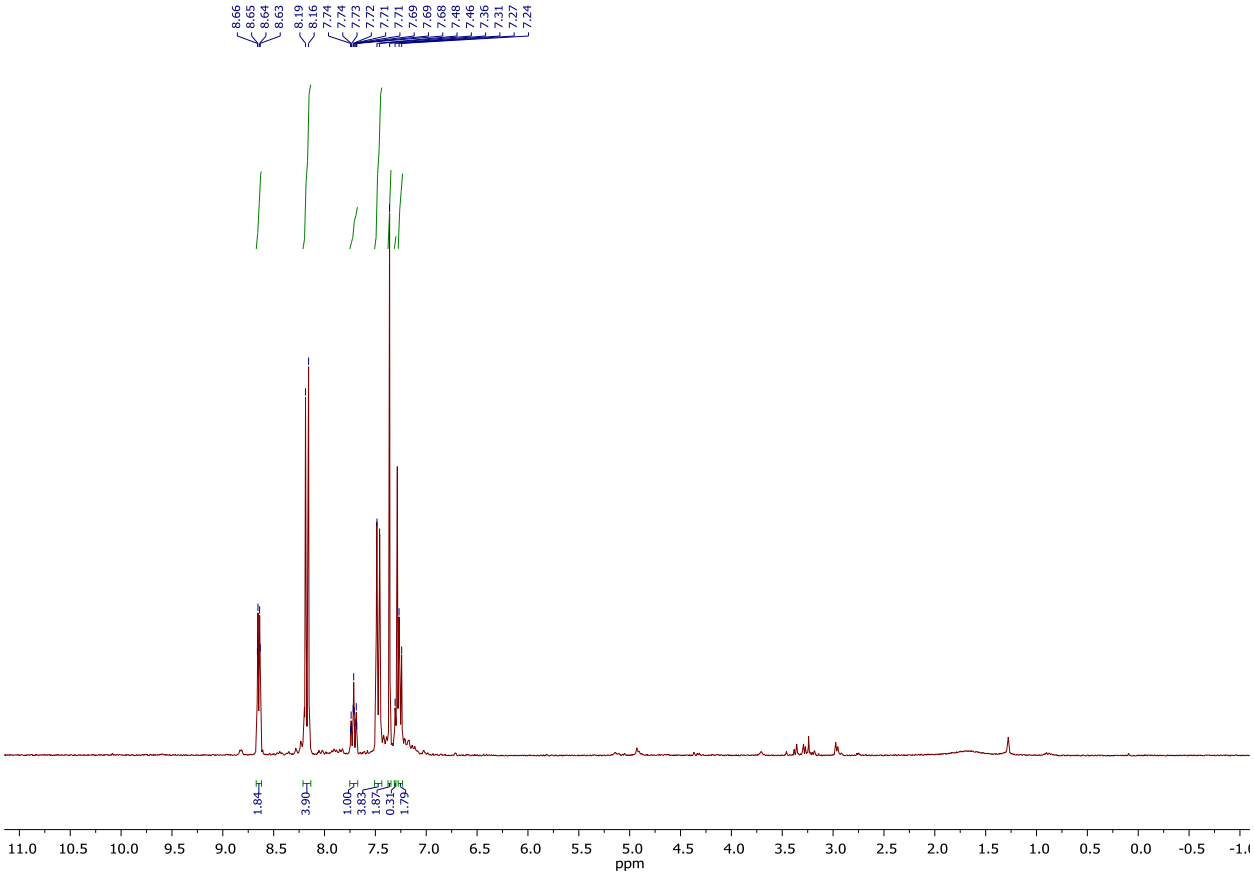

Figure S22. ^{1}H NMR spectrum of **4d**. Solvent: $CDCl_3$, 300 MHz.

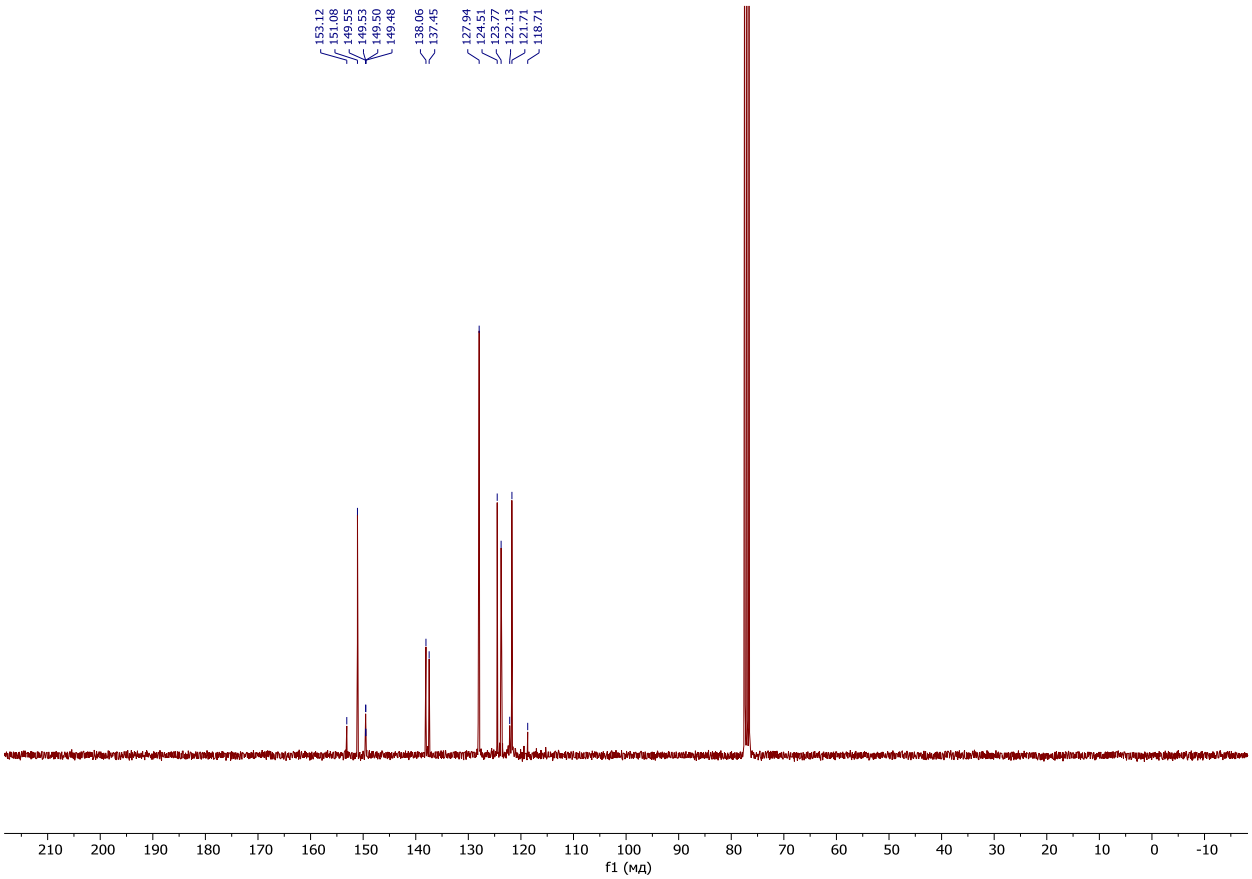

Figure S23. $^{13}C\{^{1}H\}$ NMR spectrum of **4d**. Solvent: $CDCl_3$, 75 MHz.

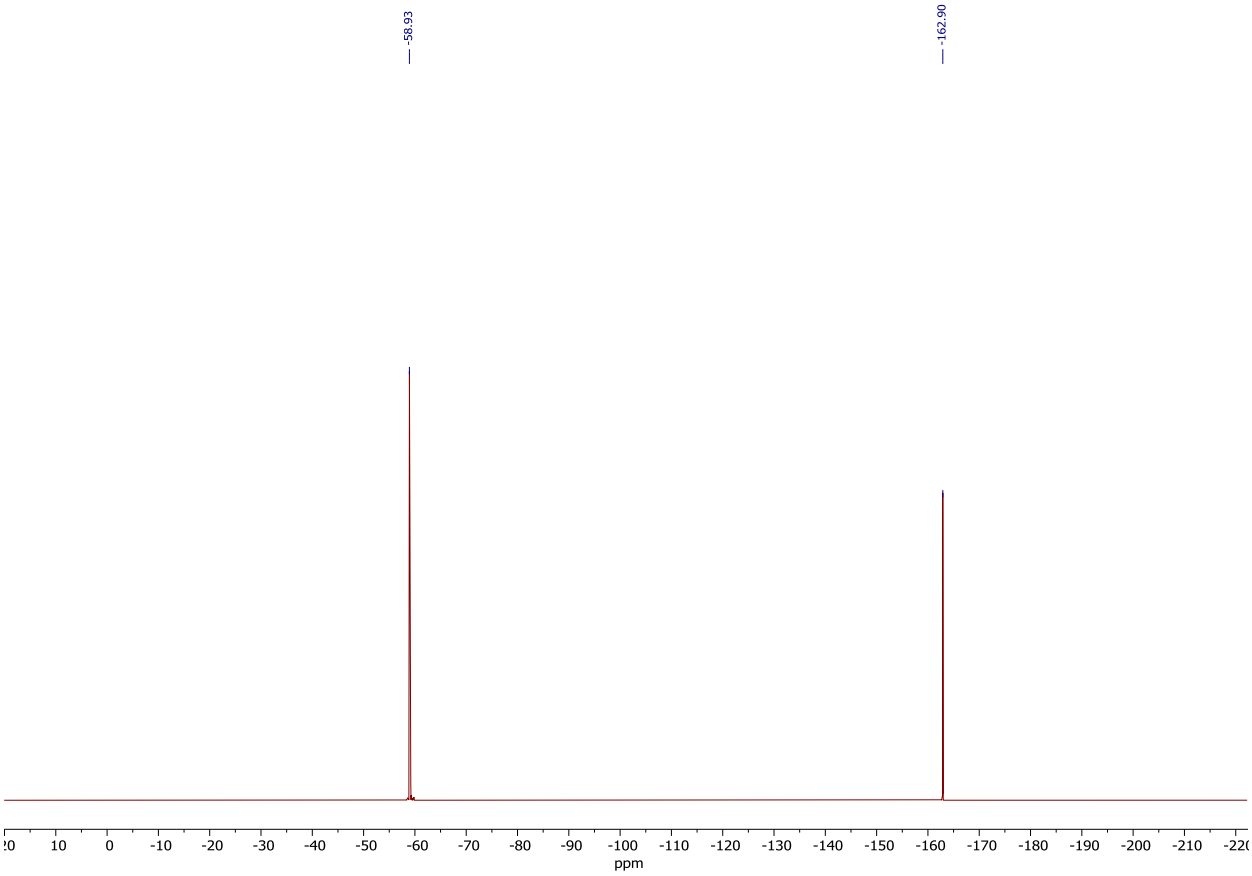

Figure S24. $^{19}F\{^{1}H\}$ NMR spectrum of **4d**. Solvent: $CDCl_3$, 282.4 MHz.. Standard: C_6F_6 with respect to $CFCl_3$.

ESI-HRMS and ESI-UHRMS spectra of the obtained compounds.

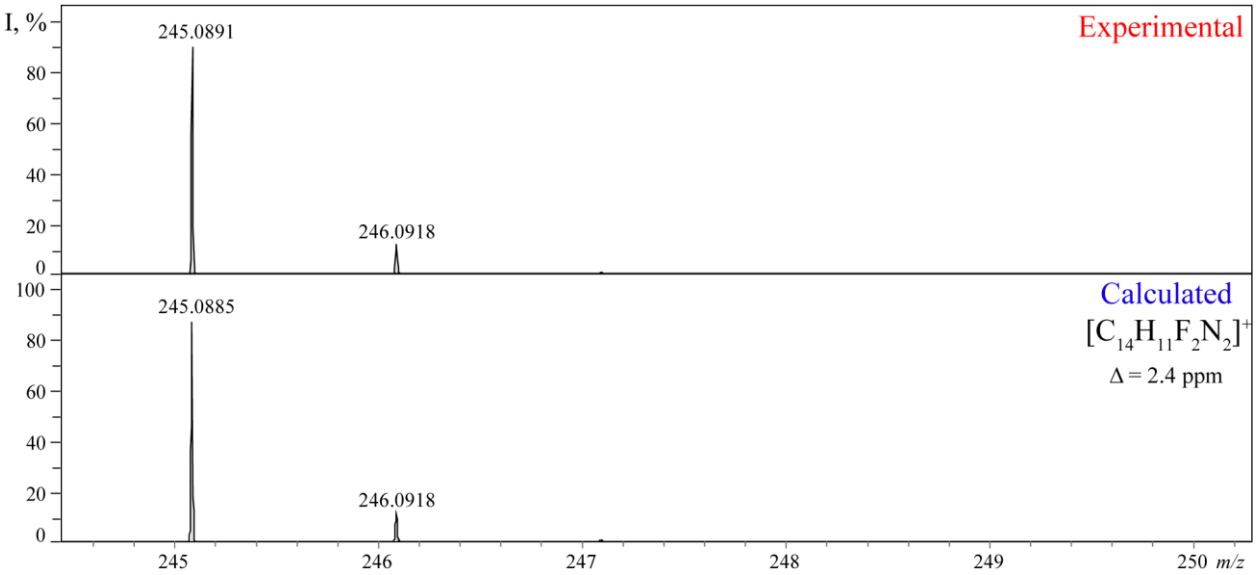

Figure S25. Experimental and theoretical ESI-(+)HRMS spectrum of **2a** in CH_3CN solution: experimental peak $[M+H]^+$ = 245.0891 Da, calculated for $C_{14}H_{11}F_2N_2$ = 245.0885, Δ = 2.4 ppm.

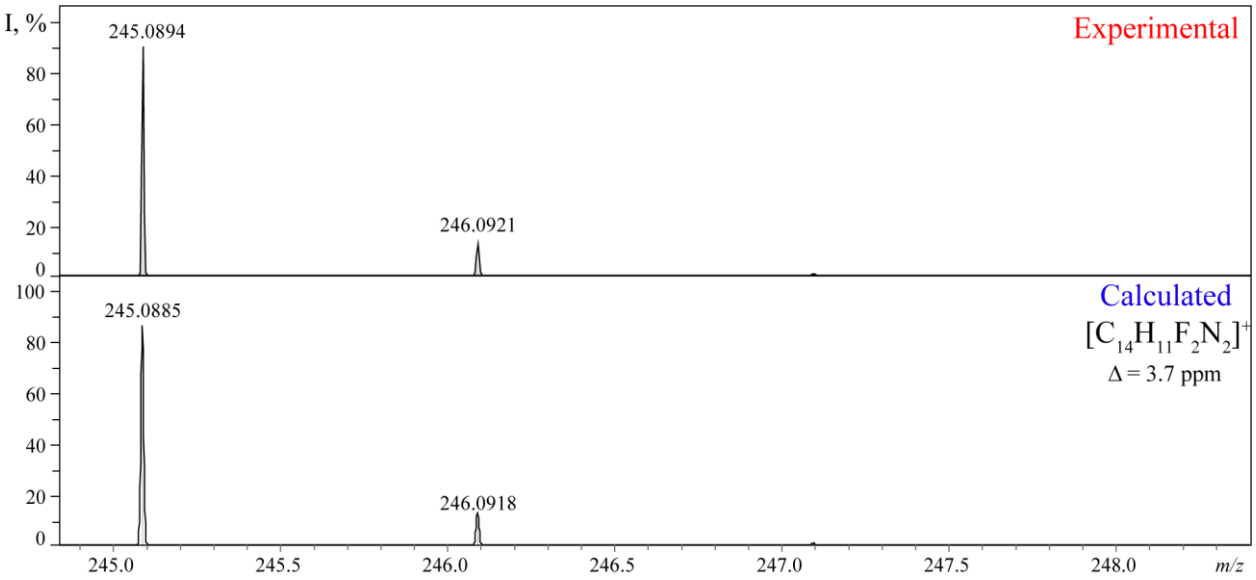

Figure S26. Experimental and theoretical ESI-(+)HRMS spectrum of **2b** in CH_3CN solution: experimental peak $[M+H]^+$ = 245.0894 Da, calculated for $C_{14}H_{11}F_2N_2$ = 245.0885, Δ = 3.7 ppm.

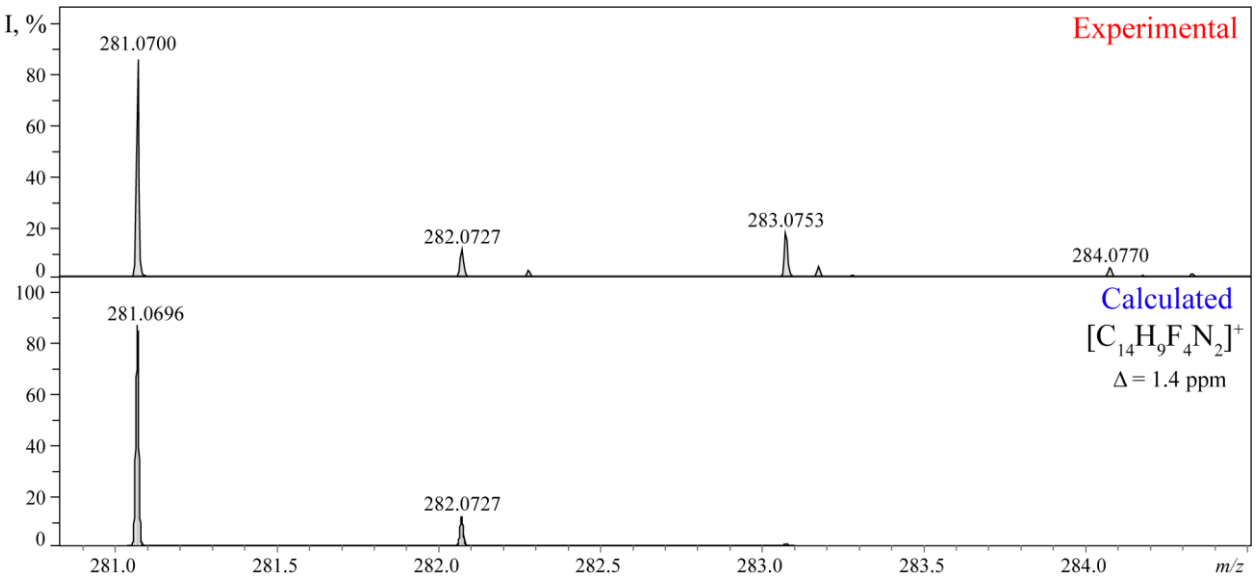

Figure S27. Experimental and theoretical ESI-(+)HRMS spectrum of **2c** in CH_3CN solution: experimental peak $[M+H]^+$ = 281.0700 Da, calculated for $C_{14}H_9F_4N_2$ = 281.0696, Δ = 1.4 ppm.

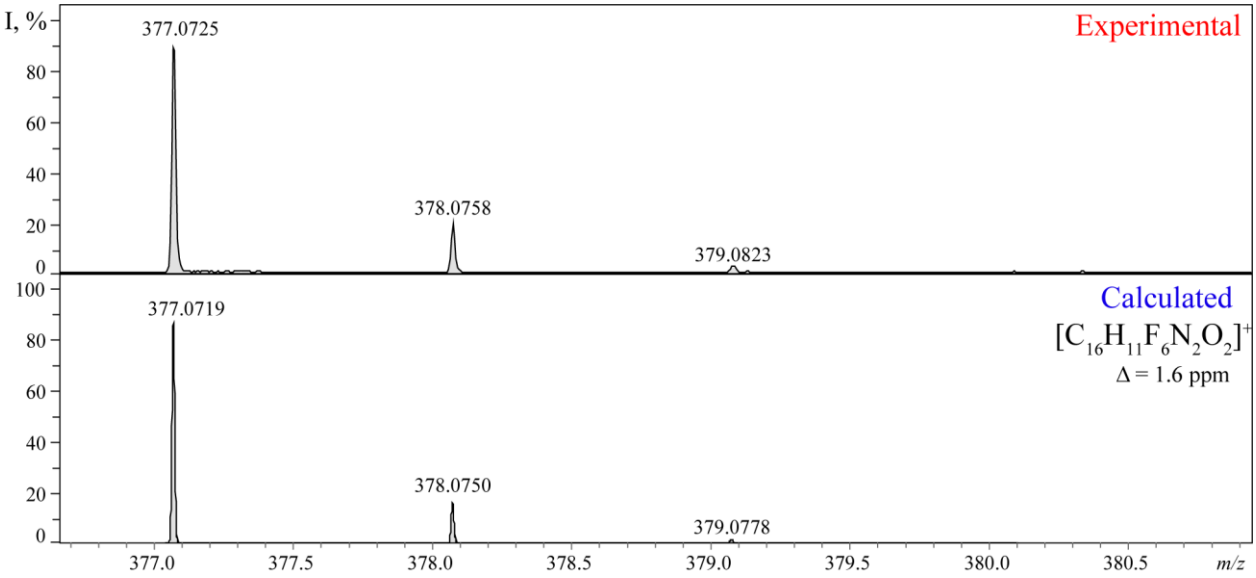

Figure S28. Experimental and theoretical ESI-(+)HRMS spectrum of **2d** in CH_3CN solution: experimental peak $[M+H]^+$ = 377.0725 Da, calculated for $C_{16}H_{11}F_6N_2O_2$ = 377.0719, Δ = 1.6 ppm.

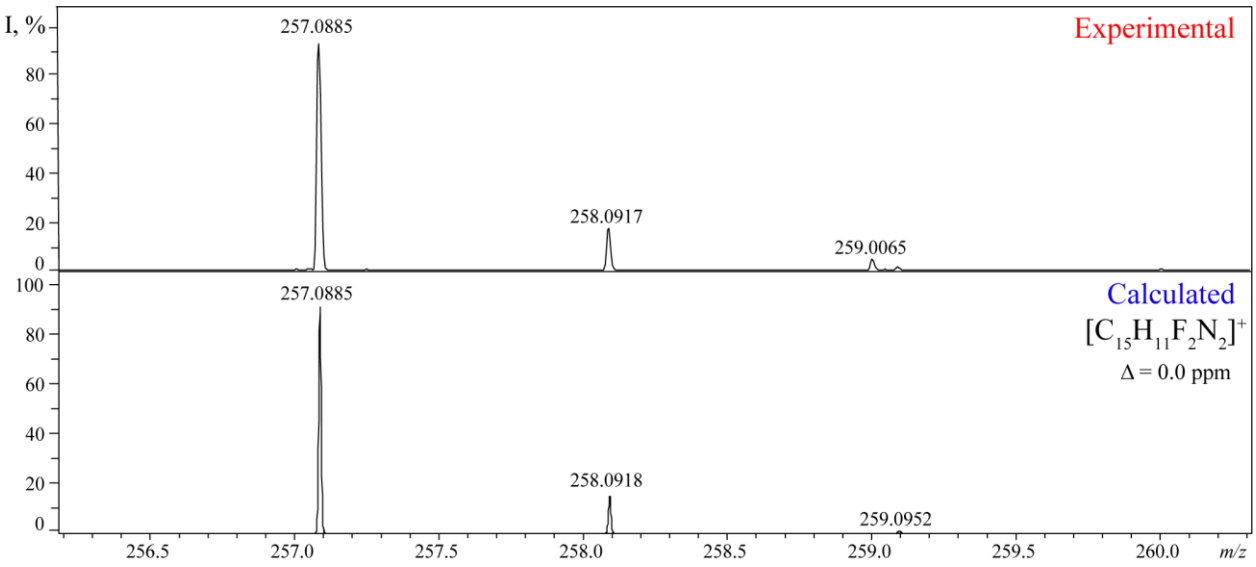

Figure S29. Experimental and theoretical ESI-(+)HRMS spectrum of **3a** in CH_3CN solution: experimental peak $[M]^+$ = 257.0885 Da, calculated for $C_{15}H_{11}F_2N_2$ = 257.0885, Δ = 0.0 ppm.

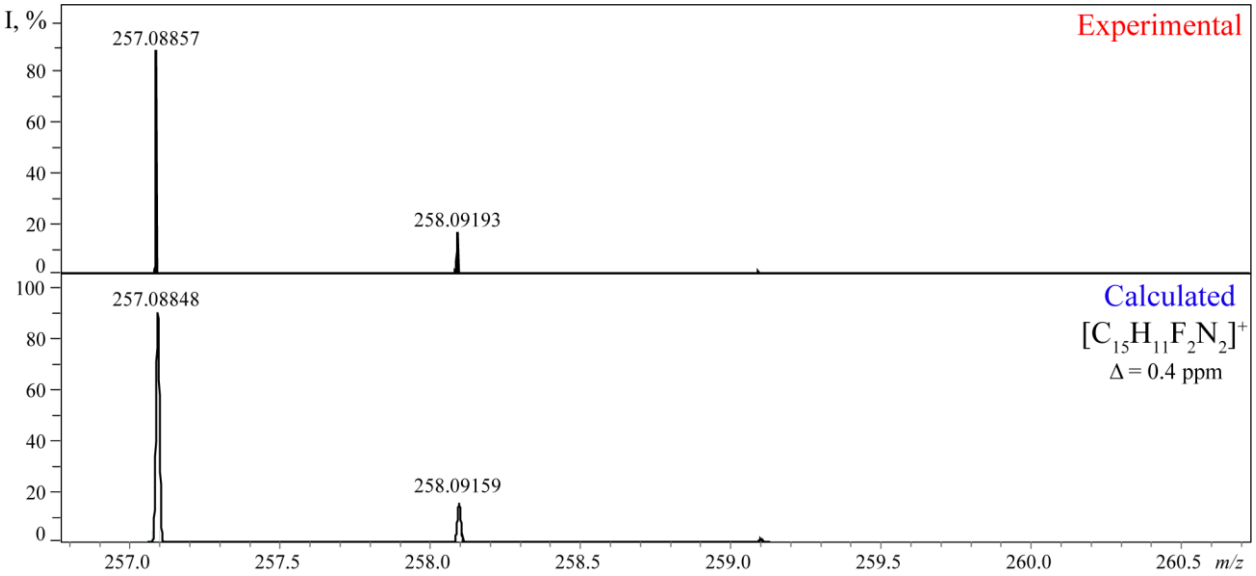

Figure S30. Experimental and theoretical ESI-(+)UHRMS spectrum of **3b** in CH_3CN solution: experimental peak $[M]^+$ = 257.08857 Da, calculated for $C_{15}H_{11}F_2N_2$ = 257.08848, Δ = 0.4 ppm.

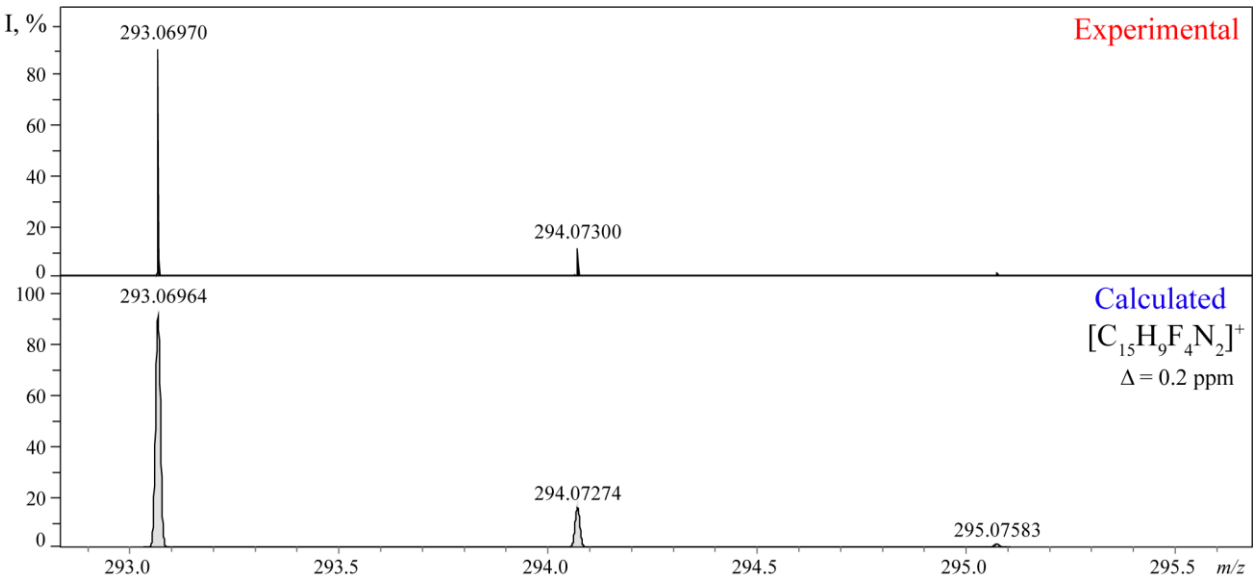

Figure S31. Experimental and theoretical ESI-(+)UHRMS spectrum of **3c** in CH_3CN solution: experimental peak $[M]^+$ = 293.06970 Da, calculated for $C_{15}H_9F_4N_2$ = 293.06964, Δ = 0.2 ppm.

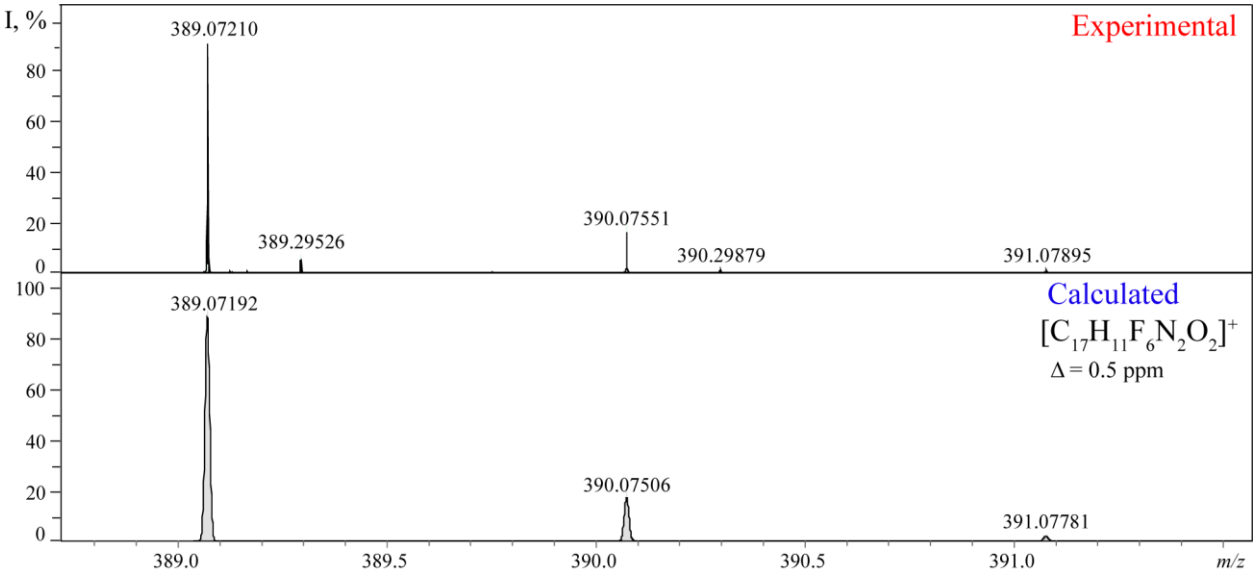

Figure S32. Experimental and theoretical ESI-(+)UHRMS spectrum of **3d** in CH_3CN solution: experimental peak $[M]^+$ = 389.07210 Da, calculated for $C_{17}H_{11}F_6N_2O_2$ = 389.07192, Δ = 0.5 ppm.

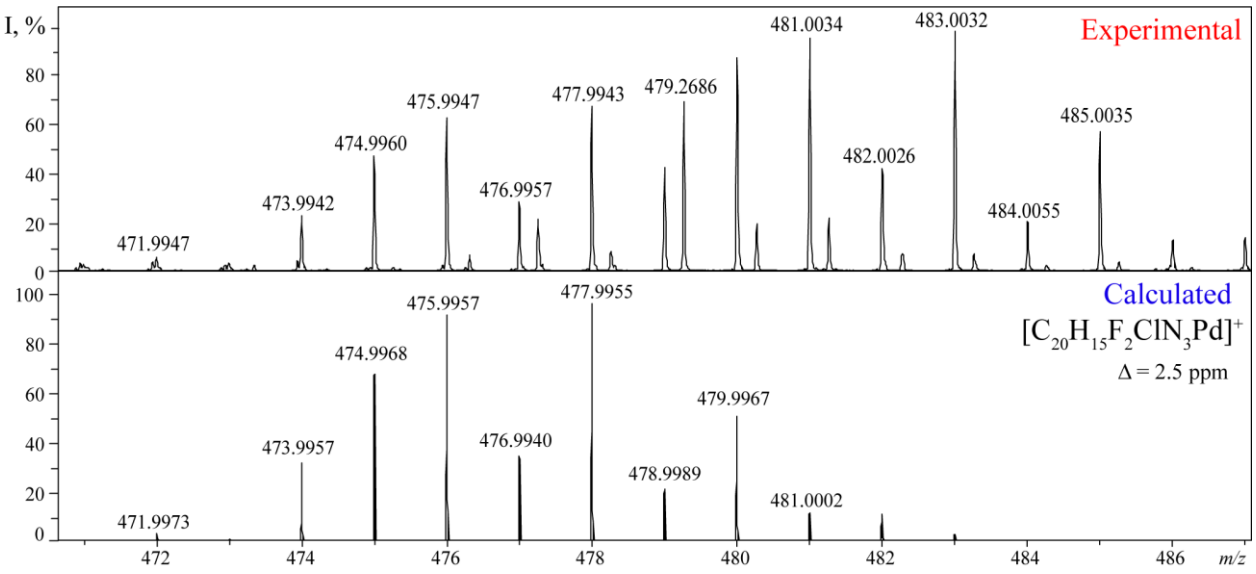

Figure S33. Experimental and theoretical ESI-(+)HRMS spectrum of **4a** in CH_3CN solution: experimental peak $[M]^+$ = 477.9943 Da, calculated for $C_{20}H_{15}F_2ClN_3Pd$ = 477.9955, Δ = 2.5 ppm.

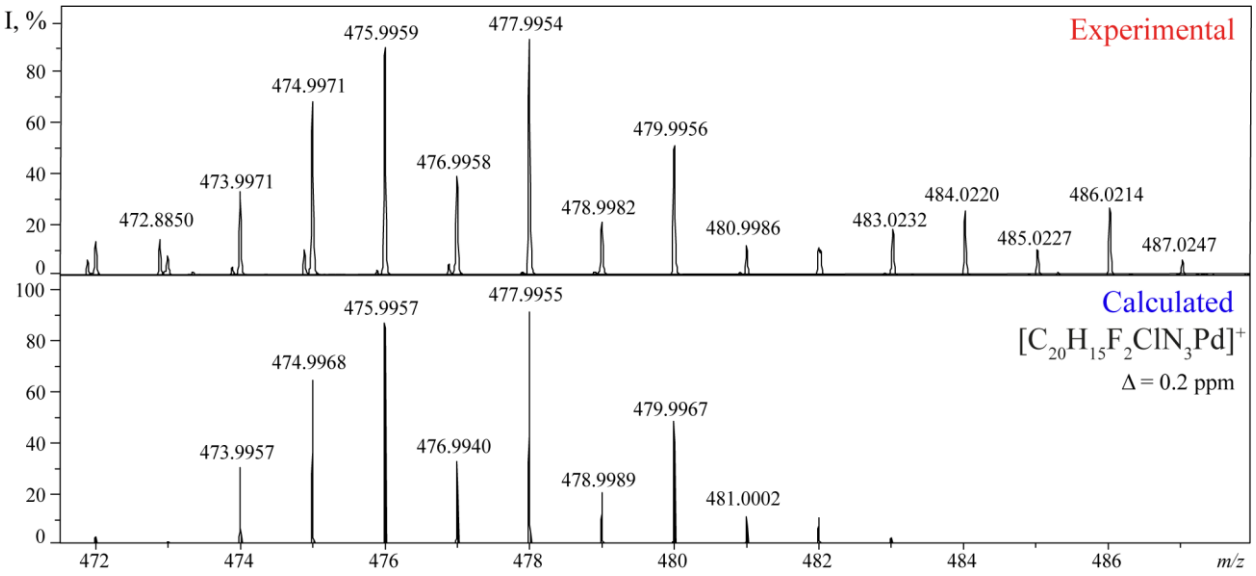

Figure S34. Experimental and theoretical ESI-(+)HRMS spectrum of **4b** in CH_3CN solution: experimental peak $[M]^+$ = 477.9954 Da, calculated for $C_{20}H_{15}F_2ClN_3Pd$ = 477.9955, Δ = 0.2 ppm.

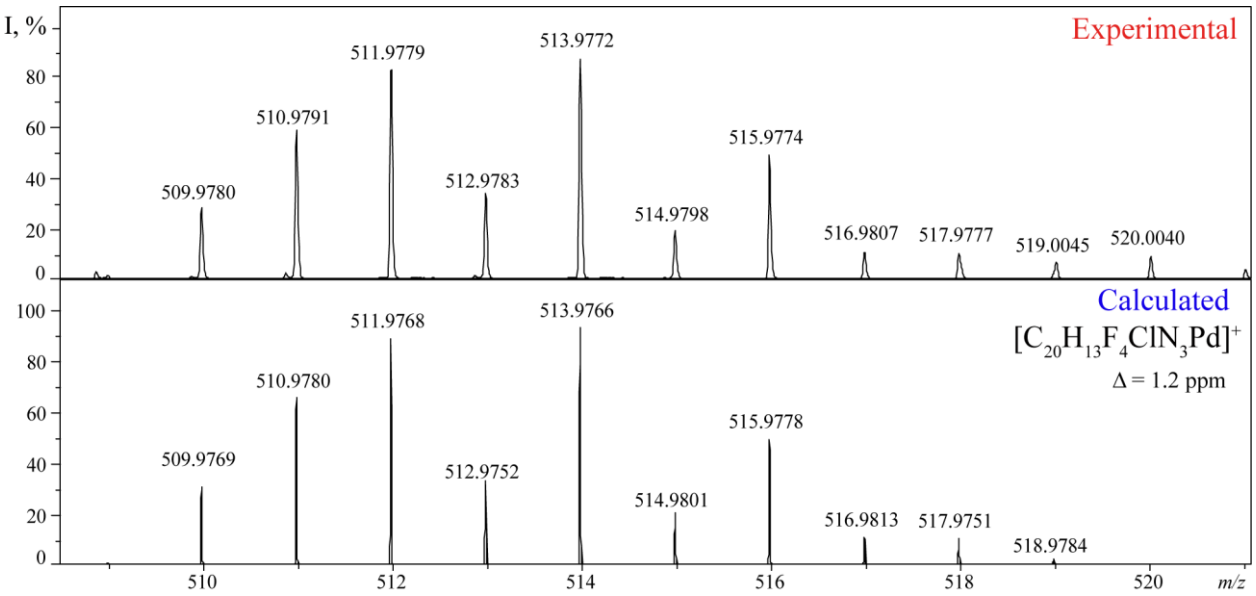

Figure S35. Experimental and theoretical ESI-(+)HRMS spectrum of **4c** in CH_3CN solution: experimental peak $[M]^+$ = 513.9772 Da, calculated for $C_{20}H_{13}F_4ClN_3Pd$ = 513.9766, Δ = 1.2 ppm.

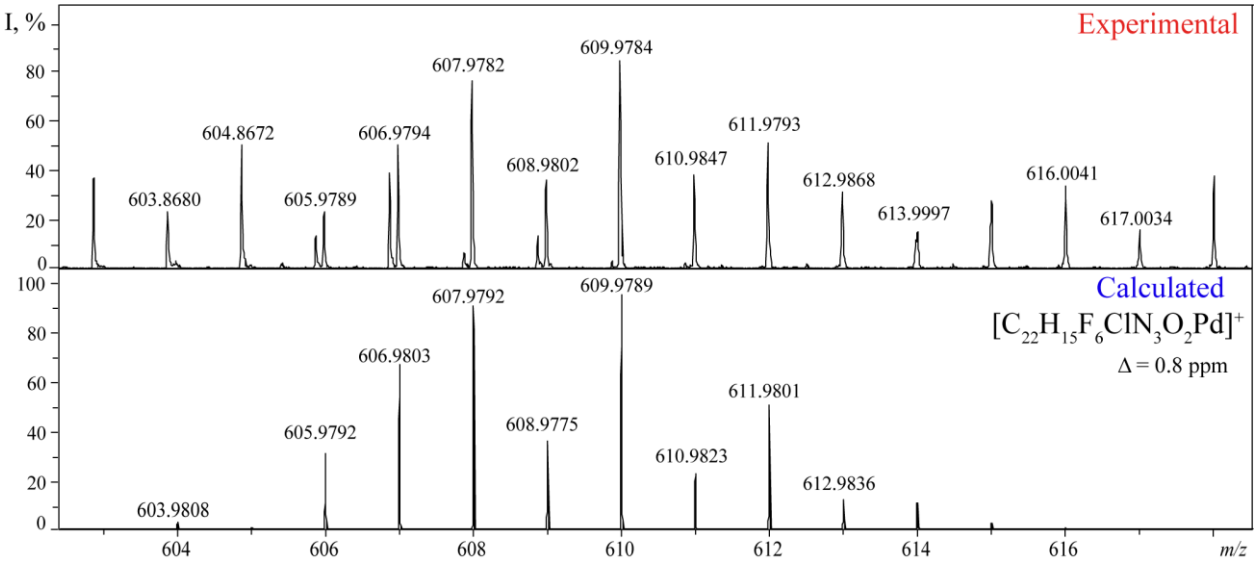

Figure S36. Experimental and theoretical ESI-(+)HRMS spectrum of **4d** in CH_3CN solution: experimental peak $[M]^+$ = 609.9784 Da, calculated for $C_{22}H_{15}F_6ClN_3O_2Pd$ = 609.9789, Δ = 0.8 ppm.

X-ray crystallographic data and refinement details

X-ray diffraction data for **3c**, **4a1**, **4a2**, **4b** and **4c** were collected at 100 K on a Rigaku Synergy S diffractometer equipped with a HyPix6000HE area detector (kappa geometry, shutterless ω-scan technique) using monochromatized Cu K_α (**3c**) or Mo K_α (**4a1**, **4a2**, **4b** and **4c**) radiation. The intensity data were integrated and corrected for absorption and decay by the CrysAlisPro program.[1] All structures were solved by direct methods using SHELXT[2] and refined on F^2 using SHELXL-2018[3] in the OLEX2 program.[4] In models **4a1**, **4a2** and **4c**, the positions of all atoms were found from the electron density-difference map; atoms were refined with individual anisotropic (nonhydrogen atoms) or isotropic (hydrogen atoms) displacement parameters. In **2a**, **3c** and highly disordered **4b**, hydrogen atoms were placed in ideal calculated positions and refined as riding atoms with relative isotropic displacement parameters. The XP program of the SHELXTL program suite[5] and the Mercury program[6] were used for molecular graphics herein and in the article, respectively.

References:

1. CrysAlisPro. Version 1.171.41.106a. *Rigaku Oxford Diffraction*, **2021**.
2. Sheldrick, G. M. SHELXT - Integrated space-group and crystal-structure determination. *Acta Cryst.* **2015**, A71, 3-8. http://doi.org/10.1107/S2053273314026370
3. Sheldrick, G. M. Crystal structure refinement with SHELXL. *Acta Cryst.* **2015**, C71, 3-8. http://doi.org/10.1107/S2053229614024218
4. Dolomanov O.V. ; Bourhis L.J. ; Gildea R.J. ; Howard J.A.K. ; Puschmann H. OLEX2: a complete structure solution, refinement and analysis program. *J. Appl. Cryst.* **2009**, 42, 229-341. http://doi.org/10.1107/S0021889808042726
5. Bruker. APEX-III. *Bruker AXS Inc.*, Madison, Wisconsin, USA, **2019**.
6. Macrae, C. F.; Sovago, I.; Cottrell, S. J.; Galek, P. T. A.; McCabe, P.; Pidcock, E.; Platings, M.; Shields, G. P.; Stevens, J. S.; Towler, M.; Wood, P. A. Mercury 4.0: from visualization to analysis, design and prediction. *J. Appl. Cryst.* 2020, **53**, 226-235. https://doi.org/10.1107/S1600576719014092

Table S1. Crystal data, data collection and structure refinement details

Identification code	**3c**	**4a1**	**4a2**	**4b**	**4c**·½CH_2Cl_2
Empirical formula	$C_{15}H_9ClF_4N_2$	$C_{20}H_{15}Cl_2F_2N_3Pd$	$C_{20}H_{15}Cl_2F_2N_3Pd$	$C_{20}H_{17}Cl_2F_2N_3Pd$	$C_{20.5}H_{14}Cl_3F_4N_3Pd$
Formula weight	328.69	512.65	512.65	514.66	591.10
Temperature (K)	100.0(1)	100.0(1)	100.0(1)	100.0(1)	100.0(1)
Wavelength (Å)	1.54184	0.71073	0.71073	0.71073	0.71073
Crystal system	Triclinic	Orthorhombic	Monoclinic	Monoclinic	Orthorhombic
Space group	$P\bar{1}$	Pbca	$P2_1/c$	C2/m	Pbcn
Unit cell dimensions					
a (Å)	6.44484(8)	11.2541(2)	9.4450(2)	6.9092(3)	22.7586(3)
b (Å)	8.57651(16)	14.2448(2)	13.5214(3)	14.7924(6)	7.15170(10)
c (Å)	12.8743(2)	24.6718(3)	31.7529(7)	9.9257(6)	26.0618(4)
α (°)	96.2904(15)	90	90	90	90
β (°)	100.2456(13)	90	93.913(2)	96.106(5)	90
γ (°)	94.1463(12)	90	90	90	90
Volume ($Å^3$)	692.98(2)	3955.20(10)	4045.70(15)	1008.69(9)	4241.89(10)
Z	2	8	8	2	8
Calcd density (g/cm^3)	1.575	1.722	1.683	1.695	1.851
μ (mm^{-1})	2.867	1.237	1.210	1.213	1.302
F(000)	332	2032	2032	512	2328
Crystal size (mm)	0.16 x 0.08 x 0.05	0.25 x 0.16 x 0.12	0.24 x 0.21 x 0.15	0.16 x 0.14 x 0.09	0.15 x 0.08 x 0.06
θ range (°)	3.516-79.572	2.450-34.992	2.161-35.000	2.754-32.493	2.376-35.498

Table S1. Crystal data, data collection and structure refinement details (cont.)

Identification code	**3c**	**4a1**	**4a2**	**4b**	**4c**·½CH_2Cl_2
Index ranges	-8<=h<=6,	-18<=h<=17,	-14<=h<=14,	-9<=h<=10,	-35<=h<=35,
	-10<=k<=10,	-22<=k<=22,	-11<=k<=21,	-22<=k<=22,	-11<=k<=8,
	-16<=l<=16	-38<=l<=39	-47<=l<=48	-14<=l<=14	-38<=l<=40
Reflections					
collected	8364	76516	41826	9325	63848
independent [R_{int}]	8364 [0.0587]	8463 [0.0503]	16449 [0.0279]	1862 [0.0370]	8926 [0.0286]
observed	7572	7332	13781	1782	7935
Completeness to $\theta_{full}/\theta_{max}$	1.000 / 0.998	1.000 / 0.973	0.999 / 0.923	0.999 /0.984	0.999 / 0.921
Data / Restraints / parameters	8364 / 0 / 200	8463 / 0 / 312	16449 / 0 / 625	1862 / 25 / 148	8926 / 0 / 341
Goodness-of-fit on F^2	1.094	1.023	1.058	1.081	1.039
R1 / wR2 [I>2σ(I)]	0.0487 / 0.1389	0.0245 / 0.0618	0.0291/ 0.0687	0.0285, 0.0735	0.0234, 0.0558
R1 / wR2 (all data)	0.0521 / 0.1427	0.0306 / 0.0642	0.0383/ 0.0720	0.0297, 0.0741	0.0279, 0.0572
$\Delta\rho_{max}$ / $\Delta\rho_{min}$ ($\bar{e}\cdot Å^{-3}$)	0.570 / -0.437	0.560 / -0.462	0.875 / -0.668	0.871 / -0.546	0.498 / -0.580
CCDC number	2131072	2131073	2131074	2131075	2131076

The structure of 3c

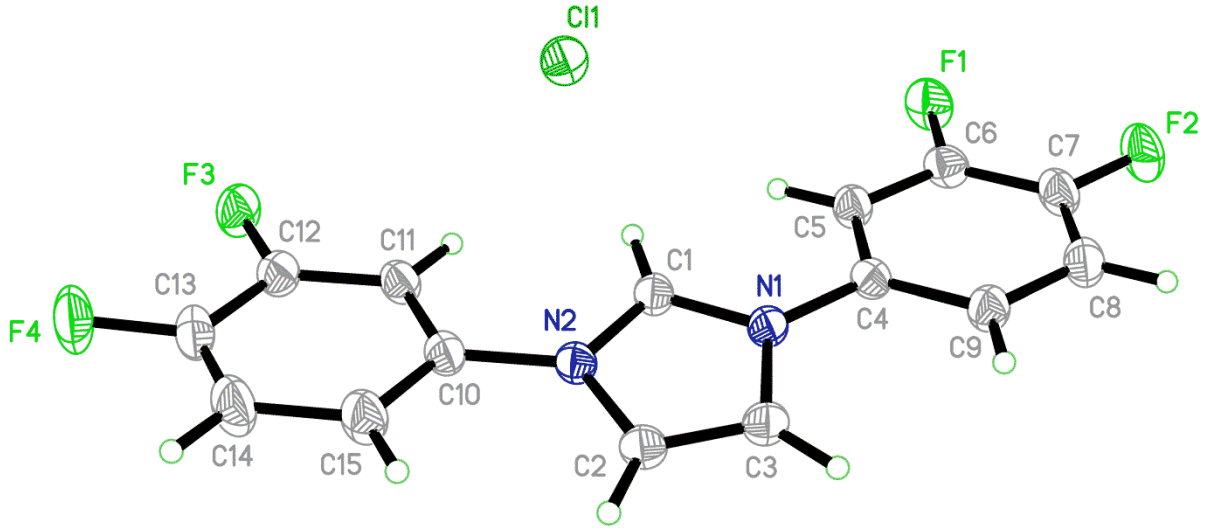

Fig. S37. The structure of **3c.**

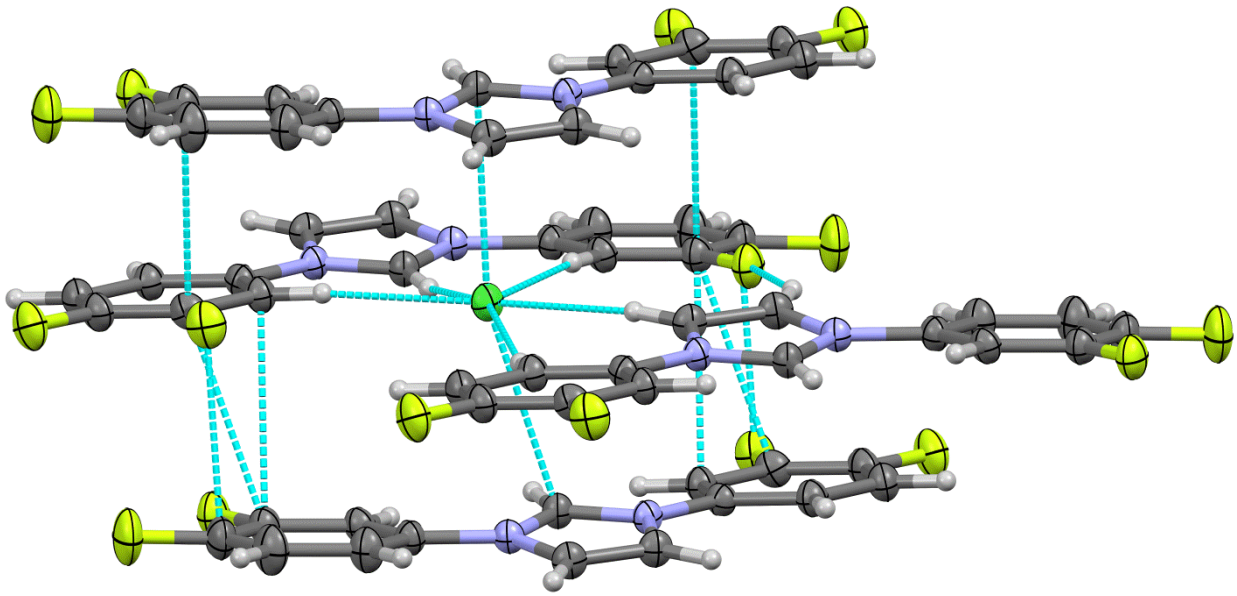

Fig. S38. The cations and anions in **3c** form layers with an interlayer distance of 3.22 Å. Short contacts are observed within the layer and between neighboring layers, including classical π-π stacking interactions.

Table S2. Selected bond distances for **3c** (Å).

Atoms	Distance	Atoms	Distance	Atoms	Distance
F(1)-C(6)	1.353(2)	N(2)-C(2)	1.387(2)	C(8)-C(9)	1.396(3)
F(2)-C(7)	1.347(2)	N(2)-C(10)	1.436(2)	C(10)-C(11)	1.394(3)
F(3)-C(12)	1.352(2)	C(2)-C(3)	1.343(3)	C(10)-C(15)	1.384(3)
F(4)-C(13)	1.352(2)	C(4)-C(5)	1.395(3)	C(11)-C(12)	1.380(3)

N(1)-C(1)	1.341(2)	C(4)-C(9)	1.397(3)	C(12)-C(13)	1.381(3)
N(1)-C(3)	1.392(2)	C(5)-C(6)	1.374(3)	C(13)-C(14)	1.368(3)
N(1)-C(4)	1.429(2)	C(6)-C(7)	1.384(3)	C(14)-C(15)	1.392(3)
N(2)-C(1)	1.331(2)	C(7)-C(8)	1.380(3)		

Table S3. Selected bond angles for **3c** (°).

Atoms	Angle	Atoms	Angle
C(1)-N(1)-C(3)	108.34(15)	F(2)-C(7)-C(6)	118.92(18)
C(1)-N(1)-C(4)	125.01(15)	F(2)-C(7)-C(8)	121.03(18)
C(3)-N(1)-C(4)	126.53(16)	C(8)-C(7)-C(6)	120.05(18)
C(1)-N(2)-C(2)	108.57(15)	C(7)-C(8)-C(9)	119.56(18)
C(1)-N(2)-C(10)	124.84(16)	C(8)-C(9)-C(4)	119.36(18)
C(2)-N(2)-C(10)	126.59(16)	C(11)-C(10)-N(2)	118.94(17)
N(2)-C(1)-N(1)	108.54(16)	C(15)-C(10)-N(2)	119.70(18)
C(3)-C(2)-N(2)	107.53(16)	C(15)-C(10)-C(11)	121.36(18)
C(2)-C(3)-N(1)	107.02(16)	C(12)-C(11)-C(10)	117.65(18)
C(5)-C(4)-N(1)	118.97(16)	F(3)-C(12)-C(11)	119.46(18)
C(5)-C(4)-C(9)	121.10(18)	F(3)-C(12)-C(13)	119.06(17)
C(9)-C(4)-N(1)	119.93(17)	C(11)-C(12)-C(13)	121.48(19)
C(6)-C(5)-C(4)	117.96(17)	F(4)-C(13)-C(14)	120.77(19)
F(1)-C(6)-C(5)	119.03(18)	C(14)-C(13)-C(12)	120.45(18)
F(1)-C(6)-C(7)	119.00(18)	C(13)-C(14)-C(15)	119.62(19)
C(5)-C(6)-C(7)	121.96(18)	C(10)-C(15)-C(14)	119.5(2)

Table S4. Torsion angles for **3c** (°).

Atoms	Angle	Atoms	Angle
F(1)-C(6)-C(7)-F(2)	-0.5(3)	C(3)-N(1)-C(4)-C(9)	-11.3(3)
F(1)-C(6)-C(7)-C(8)	-179.88(19)	C(4)-N(1)-C(1)-N(2)	176.81(16)
F(2)-C(7)-C(8)-C(9)	-178.82(19)	C(4)-N(1)-C(3)-C(2)	-176.59(17)
F(3)-C(12)-C(13)-F(4)	-1.0(3)	C(4)-C(5)-C(6)-F(1)	179.83(18)
F(3)-C(12)-C(13)-C(14)	179.9(2)	C(4)-C(5)-C(6)-C(7)	1.0(3)
F(4)-C(13)-C(14)-C(15)	-179.4(2)	C(5)-C(4)-C(9)-C(8)	0.0(3)
N(1)-C(4)-C(5)-C(6)	-179.77(17)	C(5)-C(6)-C(7)-F(2)	178.32(18)
N(1)-C(4)-C(9)-C(8)	179.29(18)	C(5)-C(6)-C(7)-C(8)	-1.1(3)
N(2)-C(2)-C(3)-N(1)	0.1(2)	C(6)-C(7)-C(8)-C(9)	0.6(3)
N(2)-C(10)-C(11)-C(12)	-179.05(18)	C(7)-C(8)-C(9)-C(4)	-0.1(3)
N(2)-C(10)-C(15)-C(14)	179.2(2)	C(9)-C(4)-C(5)-C(6)	-0.5(3)
C(1)-N(1)-C(3)-C(2)	-0.3(2)	C(10)-N(2)-C(1)-N(1)	179.02(16)
C(1)-N(1)-C(4)-C(5)	-7.7(3)	C(10)-N(2)-C(2)-C(3)	-179.22(17)

C(1)-N(1)-C(4)-C(9)	173.03(18)	C(10)-C(11)-C(12)-F(3)	-179.78(17)
C(1)-N(2)-C(2)-C(3)	0.2(2)	C(10)-C(11)-C(12)-C(13)	-0.4(3)
C(1)-N(2)-C(10)-C(11)	10.5(3)	C(11)-C(10)-C(15)-C(14)	0.0(3)
C(1)-N(2)-C(10)-C(15)	-168.66(19)	C(11)-C(12)-C(13)-F(4)	179.6(2)
C(2)-N(2)-C(1)-N(1)	-0.4(2)	C(11)-C(12)-C(13)-C(14)	0.5(3)
C(2)-N(2)-C(10)-C(11)	-170.11(19)	C(12)-C(13)-C(14)-C(15)	-0.4(4)
C(2)-N(2)-C(10)-C(15)	10.7(3)	C(13)-C(14)-C(15)-C(10)	0.1(4)
C(3)-N(1)-C(1)-N(2)	0.5(2)	C(15)-C(10)-C(11)-C(12)	0.1(3)
C(3)-N(1)-C(4)-C(5)	167.95(18)		

The C_3N_2-C_6 dihedral angles are 9.94° for C6= C4..C9 and 10.72° for C6= C10..C14, indicating a higher degree of conjugation.

The structure of 4a

Crystallization of **4a** provides two different polymorph modifications, **4a1** and **4a2**.

The structure of polymorph 4a1.

The asymmetric unit of the orthorhombic polymorph modification **4a1** contains one molecule of complex **4a**.

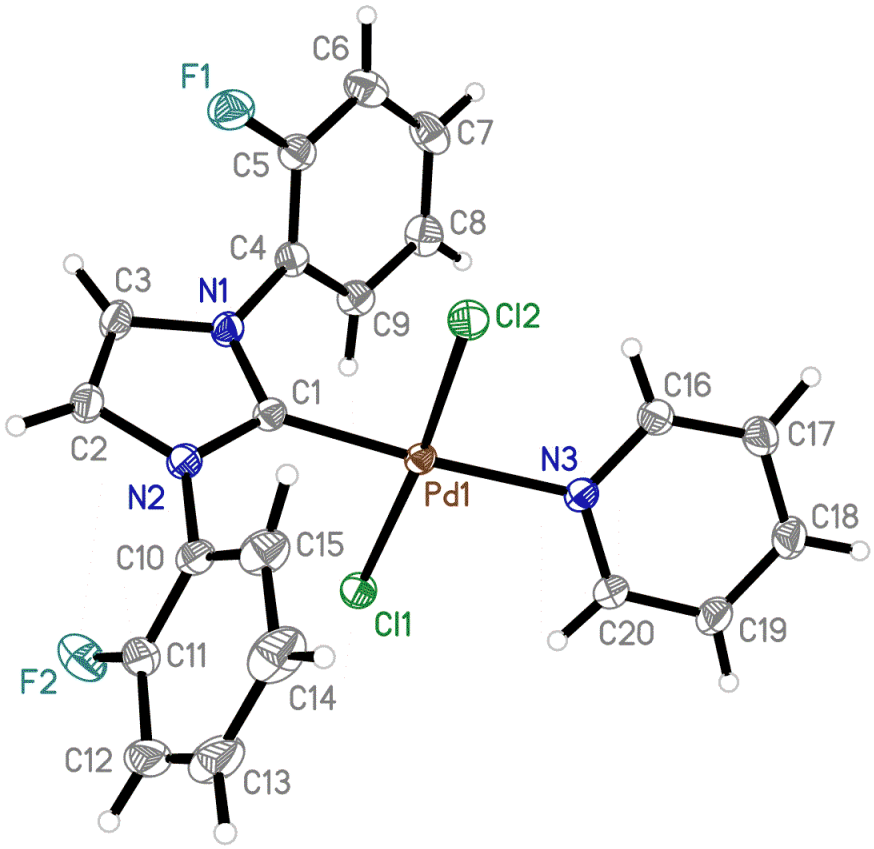

Figure S39. Crystal structure of **4a1**. Thermal ellipsoids are set to a 50% probability level.

Table S5. Selected bond distances for **4a1** (Å).

Atoms	Distance	Atoms	Distance	Atoms	Distance
Pd(1)-Cl(1)	2.3155(3)	N(2)-C(10)	1.4314(15)	C(10)-C(11)	1.3789(19)
Pd(1)-Cl(2)	2.3061(3)	N(3)-C(16)	1.3471(17)	C(10)-C(15)	1.392(2)
Pd(1)-N(3)	2.1031(10)	N(3)-C(20)	1.3428(16)	C(11)-C(12)	1.388(2)
Pd(1)-C(1)	1.9481(11)	C(2)-H(2)	0.964(19)	C(12)-C(13)	1.381(3)
F(1)-C(5)	1.3515(16)	C(2)-C(3)	1.3463(18)	C(13)-C(14)	1.384(3)
F(2)-C(11)	1.3355(19)	C(4)-C(5)	1.3829(18)	C(14)-C(15)	1.397(2)
N(1)-C(1)	1.3506(15)	C(4)-C(9)	1.3946(18)	C(16)-C(17)	1.3838(19)
N(1)-C(3)	1.3977(16)	C(5)-C(6)	1.383(2)	C(17)-C(18)	1.385(2)
N(1)-C(4)	1.4291(15)	C(6)-C(7)	1.389(2)	C(18)-C(19)	1.383(2)
N(2)-C(1)	1.3494(15)	C(7)-C(8)	1.390(2)	C(19)-C(20)	1.3891(18)
N(2)-C(2)	1.3958(16)	C(8)-C(9)	1.3919(19)		

Table S6. Selected bond angles for **4a1** (°).

Atoms	Angle	Atoms	Angle
Cl(2)-Pd(1)-Cl(1)	173.202(12)	F(1)-C(5)-C(4)	118.55(11)
N(3)-Pd(1)-Cl(1)	93.45(3)	F(1)-C(5)-C(6)	119.51(12)
N(3)-Pd(1)-Cl(2)	92.47(3)	C(6)-C(5)-C(4)	121.91(13)
C(1)-Pd(1)-Cl(1)	87.13(4)	C(5)-C(6)-C(7)	118.61(14)
C(1)-Pd(1)-Cl(2)	87.29(4)	C(6)-C(7)-C(8)	120.60(13)
C(1)-Pd(1)-N(3)	174.62(4)	C(7)-C(8)-C(9)	119.96(13)
C(1)-N(1)-C(3)	110.51(10)	C(8)-C(9)-C(4)	119.78(12)
C(1)-N(1)-C(4)	121.88(10)	C(11)-C(10)-N(2)	120.13(12)
C(3)-N(1)-C(4)	127.41(10)	C(11)-C(10)-C(15)	119.58(12)
C(1)-N(2)-C(2)	110.60(10)	C(15)-C(10)-N(2)	120.29(12)
C(1)-N(2)-C(10)	123.31(10)	F(2)-C(11)-C(10)	118.90(12)
C(2)-N(2)-C(10)	125.96(10)	F(2)-C(11)-C(12)	119.67(15)
C(16)-N(3)-Pd(1)	119.74(8)	C(10)-C(11)-C(12)	121.43(16)
C(20)-N(3)-Pd(1)	122.01(9)	C(13)-C(12)-C(11)	118.78(16)
C(20)-N(3)-C(16)	118.25(11)	C(12)-C(13)-C(14)	120.83(14)
N(1)-C(1)-Pd(1)	124.27(9)	C(13)-C(14)-C(15)	119.98(18)
N(2)-C(1)-Pd(1)	130.22(9)	C(10)-C(15)-C(14)	119.41(16)
N(2)-C(1)-N(1)	105.48(10)	N(3)-C(16)-C(17)	122.12(12)
C(3)-C(2)-N(2)	106.73(11)	C(16)-C(17)-C(18)	119.36(13)
C(2)-C(3)-N(1)	106.66(11)	C(19)-C(18)-C(17)	118.84(12)
C(5)-C(4)-N(1)	120.24(11)	C(18)-C(19)-C(20)	118.71(12)
C(5)-C(4)-C(9)	119.08(11)	N(3)-C(20)-C(19)	122.68(12)
C(9)-C(4)-N(1)	120.34(11)		

Table S7. Torsion angles for **4a1** (°).

Atoms	Angle	Atoms	Angle
Pd(1)-N(3)-C(16)-C(17)	-179.60(11)	C(4)-N(1)-C(1)-Pd(1)	-7.01(16)
Pd(1)-N(3)-C(20)-C(19)	-178.90(10)	C(4)-N(1)-C(1)-N(2)	174.84(11)
F(1)-C(5)-C(6)-C(7)	177.41(13)	C(4)-N(1)-C(3)-C(2)	-174.80(12)
F(2)-C(11)-C(12)-C(13)	178.74(13)	C(4)-C(5)-C(6)-C(7)	-0.7(2)
N(1)-C(4)-C(5)-F(1)	-6.31(18)	C(5)-C(4)-C(9)-C(8)	2.71(19)
N(1)-C(4)-C(5)-C(6)	171.82(12)	C(5)-C(6)-C(7)-C(8)	1.7(2)
N(1)-C(4)-C(9)-C(8)	-170.59(12)	C(6)-C(7)-C(8)-C(9)	-0.4(2)
N(2)-C(2)-C(3)-N(1)	0.22(15)	C(7)-C(8)-C(9)-C(4)	-1.8(2)
N(2)-C(10)-C(11)-F(2)	1.05(18)	C(9)-C(4)-C(5)-F(1)	-179.61(11)
N(2)-C(10)-C(11)-C(12)	-179.24(12)	C(9)-C(4)-C(5)-C(6)	-1.5(2)
N(2)-C(10)-C(15)-C(14)	-179.90(13)	C(10)-N(2)-C(1)-Pd(1)	6.47(18)
N(3)-C(16)-C(17)-C(18)	-1.1(2)	C(10)-N(2)-C(1)-N(1)	-175.53(11)
C(1)-N(1)-C(3)-C(2)	0.11(15)	C(10)-N(2)-C(2)-C(3)	175.46(12)
C(1)-N(1)-C(4)-C(5)	-118.30(14)	C(10)-C(11)-C(12)-C(13)	-1.0(2)
C(1)-N(1)-C(4)-C(9)	54.92(17)	C(11)-C(10)-C(15)-C(14)	0.2(2)
C(1)-N(2)-C(2)-C(3)	-0.49(16)	C(11)-C(12)-C(13)-C(14)	0.4(2)
C(1)-N(2)-C(10)-C(11)	-119.02(14)	C(12)-C(13)-C(14)-C(15)	0.4(2)
C(1)-N(2)-C(10)-C(15)	61.07(17)	C(13)-C(14)-C(15)-C(10)	-0.7(2)
C(2)-N(2)-C(1)-Pd(1)	-177.46(10)	C(15)-C(10)-C(11)-F(2)	-179.04(12)
C(2)-N(2)-C(1)-N(1)	0.54(14)	C(15)-C(10)-C(11)-C(12)	0.7(2)
C(2)-N(2)-C(10)-C(11)	65.53(17)	C(16)-N(3)-C(20)-C(19)	2.07(19)
C(2)-N(2)-C(10)-C(15)	-114.38(15)	C(16)-C(17)-C(18)-C(19)	1.3(2)
C(3)-N(1)-C(1)-Pd(1)	177.75(9)	C(17)-C(18)-C(19)-C(20)	0.2(2)
C(3)-N(1)-C(1)-N(2)	-0.40(14)	C(18)-C(19)-C(20)-N(3)	-1.9(2)
C(3)-N(1)-C(4)-C(5)	56.08(18)	C(20)-N(3)-C(16)-C(17)	-0.6(2)
C(3)-N(1)-C(4)-C(9)	-130.70(14)		

The structure of polymorph 4a2.

The asymmetric unit of monoclinic polymorph modification **4a2** contains two crystallographically inequivalent molecules of complex **4a**.

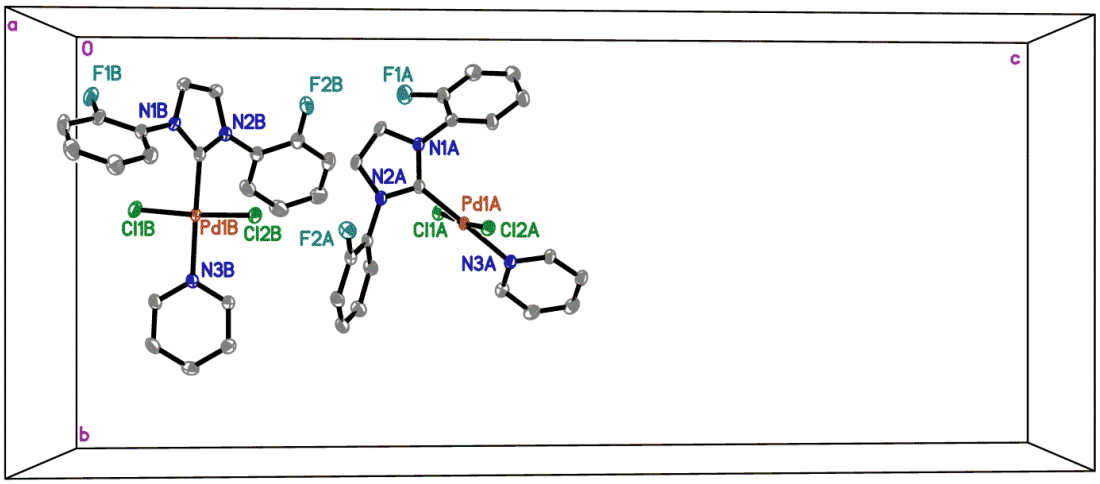

Figure S40. Unit cell and two inequivalent molecules of complex **4a** in polymorph modification **4a2**.

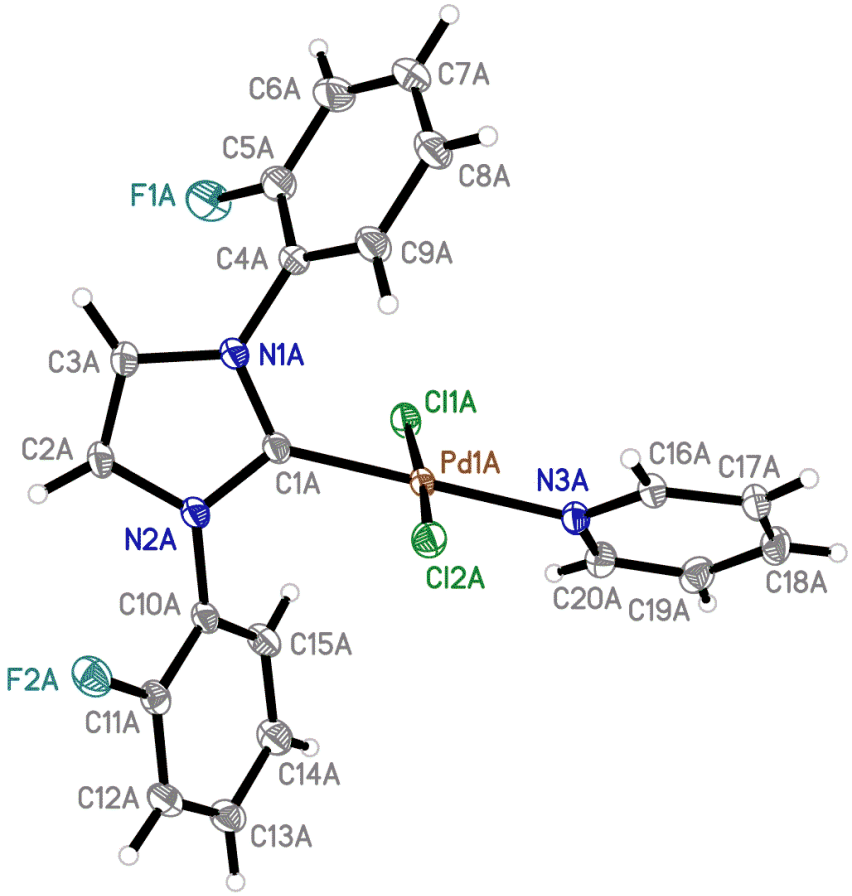

Figure S41. The structure of the first molecule of **4a** in **4a2**. Thermal ellipsoids are set to a 50% probability level.

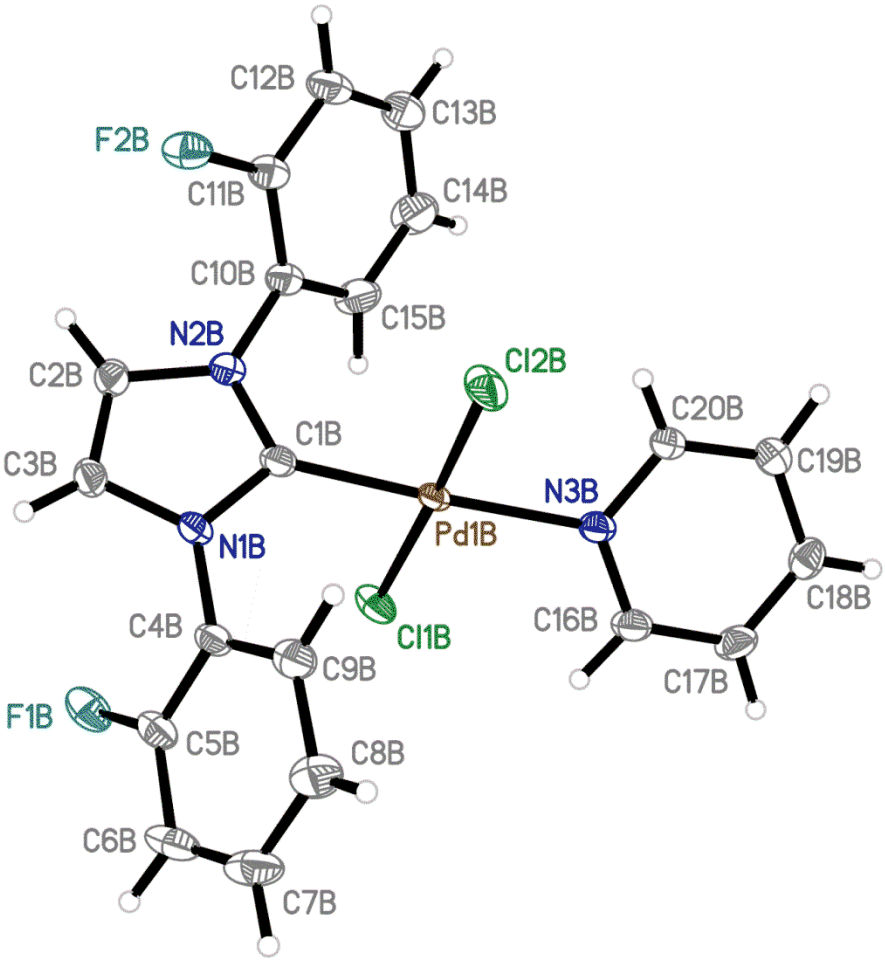

Figure S42. The structure of the second molecule of **4a** in **4a2**. Thermal ellipsoids are set to a 50% probability level.

Table S8. Selected bond distances for **4a2** (Å).

Atoms	Distance	Atoms	Distance	Atoms	Distance
Pd(1A)-Cl(1A)	2.3140(4)	C(11A)-C(12A)	1.382(2)	N(2B)-C(10B)	1.429(2)
Pd(1A)-Cl(2A)	2.3079(4)	C(12A)-C(13A)	1.382(2)	C(2B)-C(3B)	1.343(2)
Pd(1A)-C(1A)	1.9507(14)	C(13A)-C(14A)	1.387(2)	C(4B)-C(5B)	1.380(2)
Pd(1A)-N(3A)	2.0927(12)	C(14A)-C(15A)	1.385(2)	C(4B)-C(9B)	1.389(2)
F(1A)-C(5A)	1.3546(19)	N(3A)-C(16A)	1.343(2)	C(5B)-C(6B)	1.378(2)
F(2A)-C(11A)	1.3529(18)	N(3A)-C(20A)	1.343(2)	C(6B)-C(7B)	1.383(3)
N(1A)-C(1A)	1.3517(19)	C(16A)-C(17A)	1.389(2)	C(7B)-C(8B)	1.387(3)
N(1A)-C(3A)	1.3933(19)	C(17A)-C(18A)	1.386(3)	C(8B)-C(9B)	1.393(3)
N(1A)-C(4A)	1.4305(18)	C(18A)-C(19A)	1.383(3)	C(10B)-C(11B)	1.387(2)
C(1A)-N(2A)	1.3547(18)	C(19A)-C(20A)	1.386(2)	C(10B)-C(15B)	1.389(2)
N(2A)-C(2A)	1.3962(19)	Pd(1B)-Cl(1B)	2.3116(4)	C(11B)-C(12B)	1.384(2)
N(2A)-C(10A)	1.4305(19)	Pd(1B)-Cl(2B)	2.3018(4)	C(12B)-C(13B)	1.383(3)
C(2A)-C(3A)	1.344(2)	Pd(1B)-C(1B)	1.9497(15)	C(13B)-C(14B)	1.384(3)

C(4A)-C(5A)	1.381(2)	Pd(1B)-N(3B)	2.0846(13)	C(14B)-C(15B)	1.393(3)
C(4A)-C(9A)	1.388(2)	F(1B)-C(5B)	1.350(2)	N(3B)-C(16B)	1.341(2)
C(5A)-C(6A)	1.379(2)	F(2B)-C(11B)	1.3540(19)	N(3B)-C(20B)	1.349(2)
C(6A)-C(7A)	1.385(3)	N(1B)-C(1B)	1.3482(19)	C(16B)-C(17B)	1.385(2)
C(7A)-C(8A)	1.385(3)	N(1B)-C(3B)	1.397(2)	C(17B)-C(18B)	1.382(2)
C(8A)-C(9A)	1.391(2)	N(1B)-C(4B)	1.425(2)	C(18B)-C(19B)	1.388(2)
C(10A)-C(11A)	1.380(2)	C(1B)-N(2B)	1.358(2)	C(19B)-C(20B)	1.385(2)
C(10A)-C(15A)	1.387(2)	N(2B)-C(2B)	1.402(2)		

Table S9. Selected bond angles for **4a2** (°).

Atoms	Angle	Atoms	Angle
Cl(2A)-Pd(1A)-Cl(1A)	174.449(14)	C(15A)-C(10A)-N(2A)	120.63(13)
C(1A)-Pd(1A)-Cl(1A)	87.15(4)	F(2A)-C(11A)-C(10A)	118.78(13)
C(1A)-Pd(1A)-Cl(2A)	88.12(4)	N(3B)-Pd(1B)-Cl(1B)	92.77(4)
C(1A)-Pd(1A)-N(3A)	179.29(6)	N(3B)-Pd(1B)-Cl(2B)	91.11(4)
N(3A)-Pd(1A)-Cl(1A)	92.21(4)	C(1B)-N(1B)-C(3B)	110.75(13)
N(3A)-Pd(1A)-Cl(2A)	92.53(4)	C(1B)-N(1B)-C(4B)	123.27(13)
C(1A)-N(1A)-C(3A)	110.87(12)	C(3B)-N(1B)-C(4B)	125.98(13)
C(1A)-N(1A)-C(4A)	123.58(12)	N(1B)-C(1B)-Pd(1B)	127.68(11)
C(3A)-N(1A)-C(4A)	125.45(12)	N(1B)-C(1B)-N(2B)	105.28(13)
N(1A)-C(1A)-Pd(1A)	127.65(10)	N(2B)-C(1B)-Pd(1B)	126.56(11)
N(1A)-C(1A)-N(2A)	104.90(12)	C(1B)-N(2B)-C(2B)	110.38(13)
N(2A)-C(1A)-Pd(1A)	127.44(11)	C(1B)-N(2B)-C(10B)	123.36(13)
C(1A)-N(2A)-C(2A)	110.80(12)	C(2B)-N(2B)-C(10B)	126.25(13)
C(1A)-N(2A)-C(10A)	123.66(12)	C(3B)-C(2B)-N(2B)	106.63(14)
C(2A)-N(2A)-C(10A)	125.45(12)	C(2B)-C(3B)-N(1B)	106.94(13)
C(3A)-C(2A)-N(2A)	106.58(13)	C(5B)-C(4B)-N(1B)	119.83(15)
C(2A)-C(3A)-N(1A)	106.85(13)	F(2B)-C(11B)-C(12B)	119.10(15)
C(5A)-C(4A)-N(1A)	119.51(13)	C(12B)-C(11B)-C(10B)	122.37(16)
C(5A)-C(4A)-C(9A)	119.03(14)	C(13B)-C(12B)-C(11B)	118.24(17)
C(9A)-C(4A)-N(1A)	121.43(13)	C(12B)-C(13B)-C(14B)	120.56(17)
F(1A)-C(5A)-C(4A)	118.59(14)	C(13B)-C(14B)-C(15B)	120.47(18)
F(1A)-C(5A)-C(6A)	119.47(15)	C(10B)-C(15B)-C(14B)	119.69(17)
C(6A)-C(5A)-C(4A)	121.94(15)	C(16B)-N(3B)-Pd(1B)	122.53(11)
C(5A)-C(6A)-C(7A)	118.60(16)	C(16B)-N(3B)-C(20B)	118.24(14)
C(8A)-C(7A)-C(6A)	120.65(16)	C(20B)-N(3B)-Pd(1B)	119.18(10)
C(7A)-C(8A)-C(9A)	119.89(16)	N(3B)-C(16B)-C(17B)	122.38(15)
C(4A)-C(9A)-C(8A)	119.89(15)	C(18B)-C(17B)-C(16B)	119.34(15)
C(11A)-C(10A)-N(2A)	120.63(14)	C(17B)-C(18B)-C(19B)	118.69(15)

C(11A)-C(10A)-C(15A)	118.74(14)	C(20B)-C(19B)-C(18B)	118.91(15)
F(2A)-C(11A)-C(12A)	119.25(14)	N(3B)-C(20B)-C(19B)	122.44(15)
C(10A)-C(11A)-C(12A)	121.97(15)	C(5B)-C(4B)-C(9B)	119.43(15)
C(13A)-C(12A)-C(11A)	118.71(15)	C(9B)-C(4B)-N(1B)	120.70(14)
C(12A)-C(13A)-C(14A)	120.30(15)	F(1B)-C(5B)-C(4B)	118.88(15)
C(15A)-C(14A)-C(13A)	120.14(16)	F(1B)-C(5B)-C(6B)	119.04(15)
C(14A)-C(15A)-C(10A)	120.12(15)	C(6B)-C(5B)-C(4B)	122.07(17)
C(16A)-N(3A)-Pd(1A)	120.46(10)	C(5B)-C(6B)-C(7B)	118.36(17)
C(16A)-N(3A)-C(20A)	118.08(13)	C(6B)-C(7B)-C(8B)	120.69(17)
C(20A)-N(3A)-Pd(1A)	121.26(11)	C(7B)-C(8B)-C(9B)	120.22(19)
N(3A)-C(16A)-C(17A)	122.55(16)	C(4B)-C(9B)-C(8B)	119.19(16)
C(18A)-C(17A)-C(16A)	118.81(16)	C(11B)-C(10B)-N(2B)	120.52(14)
C(19A)-C(18A)-C(17A)	118.92(15)	C(11B)-C(10B)-C(15B)	118.56(15)
C(18A)-C(19A)-C(20A)	118.87(16)	C(15B)-C(10B)-N(2B)	120.86(15)
N(3A)-C(20A)-C(19A)	122.70(15)	F(2B)-C(11B)-C(10B)	118.52(14)
Cl(2B)-Pd(1B)-Cl(1B)	174.388(16)	C(1B)-Pd(1B)-Cl(2B)	90.41(5)
C(1B)-Pd(1B)-Cl(1B)	86.01(5)	C(1B)-Pd(1B)-N(3B)	175.64(6)

Table S10. Torsion angles for **4a2** (°).

Atoms	Angle	Atoms	Angle
Pd(1A)-C(1A)-N(2A)-C(2A)	-179.35(11)	C(3A)-N(1A)-C(4A)-C(9A)	123.96(17)
Pd(1A)-C(1A)-N(2A)-C(10A)	-2.7(2)	C(4A)-N(1A)-C(1A)-Pd(1A)	2.8(2)
Pd(1A)-N(3A)-C(16A)-C(17A)	-172.55(12)	C(4A)-N(1A)-C(1A)-N(2A)	-176.58(13)
Pd(1A)-N(3A)-C(20A)-C(19A)	174.06(12)	C(4A)-N(1A)-C(3A)-C(2A)	176.43(14)
F(1A)-C(5A)-C(6A)-C(7A)	-179.42(17)	C(4A)-C(5A)-C(6A)-C(7A)	-0.2(3)
F(2A)-C(11A)-C(12A)-C(13A)	-178.11(14)	C(5A)-C(4A)-C(9A)-C(8A)	0.8(3)
N(1A)-C(1A)-N(2A)-C(2A)	0.02(17)	C(5A)-C(6A)-C(7A)-C(8A)	0.4(3)
N(1A)-C(1A)-N(2A)-C(10A)	176.69(13)	C(6A)-C(7A)-C(8A)-C(9A)	0.0(3)
N(1A)-C(4A)-C(5A)-F(1A)	0.6(2)	C(7A)-C(8A)-C(9A)-C(4A)	-0.6(3)
N(1A)-C(4A)-C(5A)-C(6A)	-178.62(16)	C(9A)-C(4A)-C(5A)-F(1A)	178.81(15)
N(1A)-C(4A)-C(9A)-C(8A)	178.97(16)	C(9A)-C(4A)-C(5A)-C(6A)	-0.4(3)
C(1A)-N(1A)-C(3A)-C(2A)	-0.13(18)	C(10A)-N(2A)-C(2A)-C(3A)	-176.70(14)
C(1A)-N(1A)-C(4A)-C(5A)	118.24(17)	C(10A)-C(11A)-C(12A)-C(13A)	1.3(2)
C(1A)-N(1A)-C(4A)-C(9A)	-59.9(2)	C(11A)-C(10A)-C(15A)-C(14A)	-1.5(2)
C(1A)-N(2A)-C(2A)-C(3A)	-0.10(18)	C(11A)-C(12A)-C(13A)-C(14A)	-1.5(2)
C(1A)-N(2A)-C(10A)-C(11A)	128.78(16)	C(12A)-C(13A)-C(14A)-C(15A)	0.3(3)
C(1A)-N(2A)-C(10A)-C(15A)	-50.5(2)	C(13A)-C(14A)-C(15A)-C(10A)	1.2(3)
N(2A)-C(2A)-C(3A)-N(1A)	0.14(18)	C(15A)-C(10A)-C(11A)-F(2A)	179.62(14)
N(2A)-C(10A)-C(11A)-F(2A)	0.3(2)	C(15A)-C(10A)-C(11A)-C(12A)	0.2(2)

N(2A)-C(10A)-C(11A)-C(12A)	-179.12(14)	N(3A)-C(16A)-C(17A)-C(18A)	-1.7(2)
N(2A)-C(10A)-C(15A)-C(14A)	177.87(15)	C(16A)-N(3A)-C(20A)-C(19A)	-0.9(2)
C(2A)-N(2A)-C(10A)-C(11A)	-55.0(2)	C(16A)-C(17A)-C(18A)-C(19A)	-0.6(2)
C(2A)-N(2A)-C(10A)-C(15A)	125.63(17)	C(17A)-C(18A)-C(19A)-C(20A)	2.0(2)
C(3A)-N(1A)-C(1A)-Pd(1A)	179.43(11)	C(18A)-C(19A)-C(20A)-N(3A)	-1.3(3)
C(3A)-N(1A)-C(1A)-N(2A)	0.06(17)	C(20A)-N(3A)-C(16A)-C(17A)	2.5(2)
C(3A)-N(1A)-C(4A)-C(5A)	-57.9(2)	Pd(1B)-C(1B)-N(2B)-C(2B)	171.95(11)
Pd(1B)-C(1B)-N(2B)-C(10B)	-9.2(2)	C(1B)-N(1B)-C(4B)-C(9B)	50.2(2)
Pd(1B)-N(3B)-C(16B)-C(17B)	178.17(14)	C(1B)-N(2B)-C(2B)-C(3B)	0.11(18)
Pd(1B)-N(3B)-C(20B)-C(19B)	-177.41(13)	C(1B)-N(2B)-C(10B)-C(11B)	-124.61(17)
F(1B)-C(5B)-C(6B)-C(7B)	176.04(15)	C(1B)-N(2B)-C(10B)-C(15B)	52.6(2)
F(2B)-C(11B)-C(12B)-C(13B)	-177.70(17)	N(2B)-C(2B)-C(3B)-N(1B)	0.44(17)
N(1B)-C(1B)-N(2B)-C(2B)	-0.63(17)	N(2B)-C(10B)-C(11B)-F(2B)	-6.5(2)
N(1B)-C(1B)-N(2B)-C(10B)	178.20(14)	N(2B)-C(10B)-C(11B)-C(12B)	173.42(16)
N(1B)-C(4B)-C(5B)-F(1B)	0.5(2)	N(2B)-C(10B)-C(15B)-C(14B)	-174.79(18)
N(1B)-C(4B)-C(5B)-C(6B)	179.04(15)	C(2B)-N(2B)-C(10B)-C(11B)	54.0(2)
N(1B)-C(4B)-C(9B)-C(8B)	-177.21(15)	C(2B)-N(2B)-C(10B)-C(15B)	-128.72(19)
C(1B)-N(1B)-C(3B)-C(2B)	-0.87(18)	C(3B)-N(1B)-C(1B)-Pd(1B)	-171.55(12)
C(1B)-N(1B)-C(4B)-C(5B)	-127.64(16)	C(3B)-N(1B)-C(1B)-N(2B)	0.92(17)
C(3B)-N(1B)-C(4B)-C(5B)	51.7(2)	C(10B)-N(2B)-C(2B)-C(3B)	-178.68(15)
C(3B)-N(1B)-C(4B)-C(9B)	-130.37(17)	C(10B)-C(11B)-C(12B)-C(13B)	2.4(3)
C(4B)-N(1B)-C(1B)-Pd(1B)	7.9(2)	C(11B)-C(10B)-C(15B)-C(14B)	2.5(3)
C(4B)-N(1B)-C(1B)-N(2B)	-179.62(14)	C(11B)-C(12B)-C(13B)-C(14B)	0.5(3)
C(4B)-N(1B)-C(3B)-C(2B)	179.68(14)	C(12B)-C(13B)-C(14B)-C(15B)	-1.8(4)
C(4B)-C(5B)-C(6B)-C(7B)	-2.5(3)	C(13B)-C(14B)-C(15B)-C(10B)	0.2(3)
C(5B)-C(4B)-C(9B)-C(8B)	0.7(2)	C(15B)-C(10B)-C(11B)-F(2B)	176.20(16)
C(5B)-C(6B)-C(7B)-C(8B)	2.1(3)	C(15B)-C(10B)-C(11B)-C(12B)	-3.9(3)
C(6B)-C(7B)-C(8B)-C(9B)	-0.3(3)	N(3B)-C(16B)-C(17B)-C(18B)	-1.0(3)
C(7B)-C(8B)-C(9B)-C(4B)	-1.1(3)	C(16B)-N(3B)-C(20B)-C(19B)	-0.1(3)
C(9B)-C(4B)-C(5B)-F(1B)	-177.42(14)	C(16B)-C(17B)-C(18B)-C(19B)	0.2(3)
C(9B)-C(4B)-C(5B)-C(6B)	1.1(2)	C(17B)-C(18B)-C(19B)-C(20B)	0.6(3)
C(18B)-C(19B)-C(20B)-N(3B)	-0.7(3)	C(20B)-N(3B)-C(16B)-C(17B)	0.9(3)

The structure of 4b

Better refinement results for **4b** were obtained in the C2/m space group rather than in C2. Other space groups were also tested.

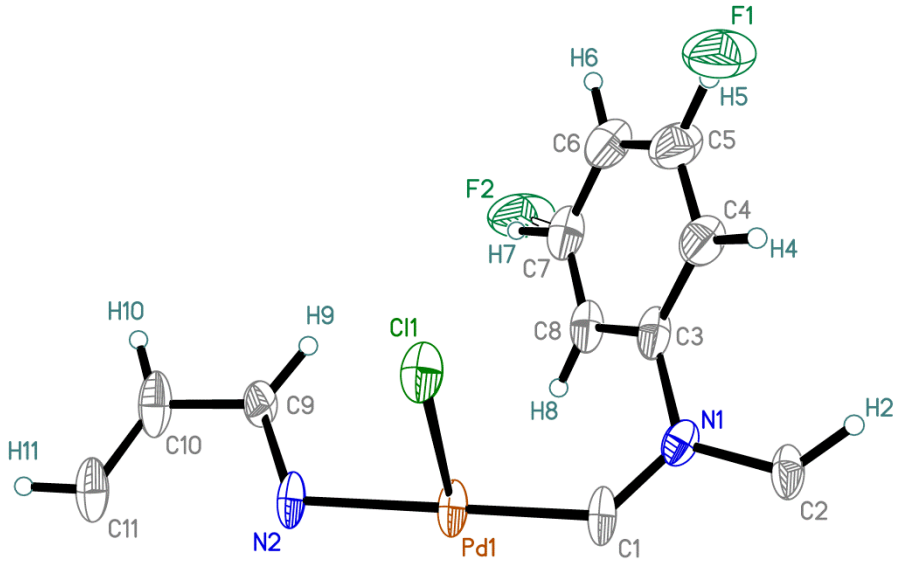

Figure S43. Crystallographically inequivalent fragment of the molecule **4b**. Thermal ellipsoids are set to a 50% probability level.

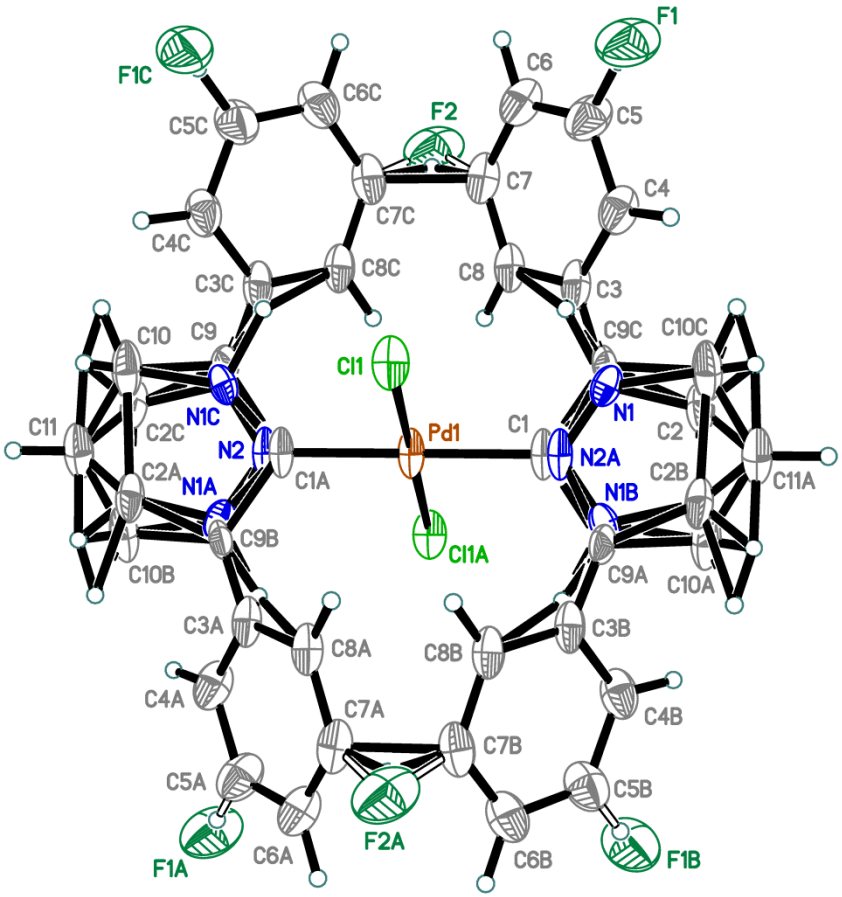

Figure S44. The real structure of **4b**, which is superposition of two equivalent molecules **4b**. Thermal ellipsoids are set to a 50% probability level.

Atom Pd1 is located at an inversion center; atoms Pd1, Cl1, C1, N2 and C11 are situated on a mirror plane. The occupancy of atoms Pd1, C1, N2 and C11 situated on a mirror plane is 0.25, other atoms (except for disordered H7/F2 and H5/F1 fragments) have occupancy of 0.5. Therefore, half the molecule **4b** is crystallographically unique (Fig. S43) and Z'=¼.

The overall structure with symmetry generated atoms is shown in Fig. S44, which is the result of a superposition of two equivalent molecules (shown in Fig. S45) both having occupancies of 0.5. Additionally, the fluorine atom is disordered over two positions (Fig. S45). The structure of the complex with omitted disorder is shown in Fig. S46.

A relatively poor precision in determining bond lengths is likely because the asymmetric unit is fully disordered over four positions. Unfortunately, further modeling, where atoms N2, C1, and C11 were slightly out of the crystallographic mirror plane, did not provide a better crystallographic model for **4b**.

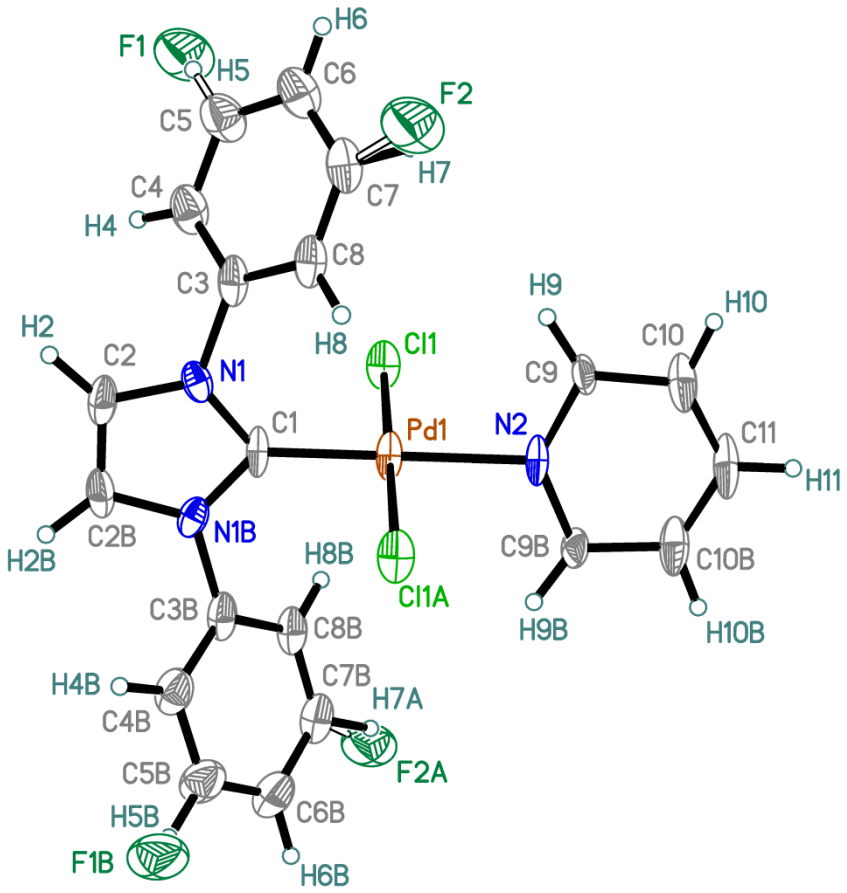

Figure S45. The structure of complex **4b** (occupancy is 0.5). The thermal ellipsoids are set to a 50% probability level. The disorder ratio for atoms H7/F2 and F1/H5 is 0.896(5):0.104(5).

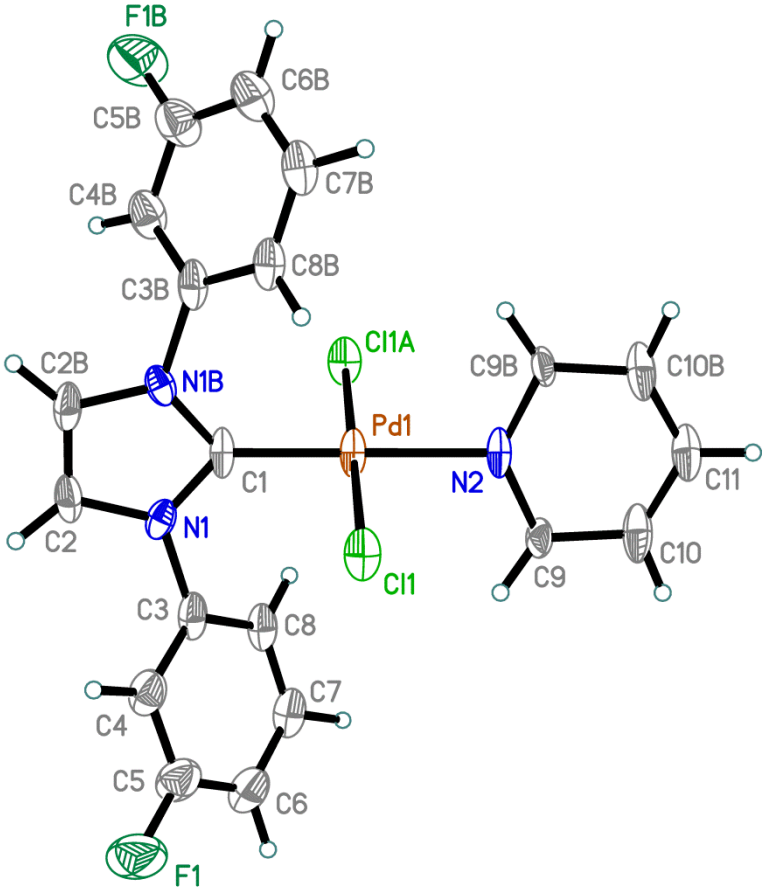

Figure S46. The structure of complex **4b**. The thermal ellipsoids are set to a 50% probability level. The fluorine disorder is not shown for clarity.

Table S11. Selected bond distances for **4b** (Å).

Atoms	Distance	Atoms	Distance	Atoms	Distance
Pd(1)-Cl(1)	2.3176(6)	C(3)-C(8)	1.389(5)	C(7)-F(2)	1.320(6)
Pd(1)-C(1)	1.88(3)	C(4)-H(4)	0.976(10)	C(7)-C(8)	1.390(6)
Pd(1)-N(2)	2.12(2)	C(4)-C(5)	1.387(6)	C(8)-H(8)	0.975(10)
C(1)-N(1)	1.31(2)	C(5)-H(5)	0.980(10)	N(2)-C(9)	1.404(17)
N(1)-C(2)	1.353(12)	C(5)-F(1)	1.325(6)	C(9)-H(9)	0.978(10)
N(1)-C(3)	1.530(11)	C(5)-C(6)	1.374(6)	C(9)-C(10)	1.443(13)
C(2)-C(2)#1	1.343(12)	C(6)-H(6)	0.973(10)	C(10)-H(10)	0.980(10)
C(2)-H(2)	0.974(10)	C(6)-C(7)	1.384(6)	C(10)-C(11)	1.377(7)
C(3)-C(4)	1.389(6)	C(7)-H(7)	1.105(9)	C(11)-H(11)	0.981(10)

Symmetry transformation to generate equivalent atoms: #1 -x+1, y, -z+1

Table S12. Selected bond angles for **4b** (°).

Atoms	Angle	Atoms	Angle
Cl(1)#2-Pd(1)-Cl(1)	180.00(3)	F(1)-C(5)-C(4)	117.0(4)
C(1)-Pd(1)-Cl(1)	90.000(1)	F(1)-C(5)-C(6)	120.2(4)
C(1)-Pd(1)-N(2)	180.0	C(6)-C(5)-C(4)	122.7(4)
N(2)-Pd(1)-Cl(1)	90.000(2)	C(5)-C(6)-C(7)	118.4(4)
N(1)-C(1)-Pd(1)	132.0(10)	C(6)-C(7)-C(8)	121.1(3)
C(1)-N(1)-C(2)	119.0(12)	F(2)-C(7)-C(6)	109.5(8)
C(1)-N(1)-C(3)	120.5(11)	F(2)-C(7)-C(8)	128.7(9)
C(2)-N(1)-C(3)	120.3(8)	C(3)-C(8)-C(7)	118.8(3)
C(2)#1-C(2)-N(1)	102.9(5)	C(9)-N(2)-Pd(1)	116.0(9)
C(4)-C(3)-N(1)	117.1(5)	C(9)#1-N(2)-C(9)	128.0(19)
C(8)-C(3)-N(1)	121.5(5)	N(2)-C(9)-C(10)	113.0(12)
C(8)-C(3)-C(4)	121.3(4)	C(11)-C(10)-C(9)	123.3(7)
C(5)-C(4)-C(3)	117.6(4)	C(10)-C(11)-C(10)#1	119.2(6)

Symmetry transformations to generate equivalent atoms: #1 -x+1, y, -z+1; #2 -x+1, -y+1, -z+1

Table S13. Torsion angles for **4b** (°).

Atoms	Angle	Atoms	Angle
Pd(1)-C(1)-N(1)-C(2)	-178.5(4)	C(3)-N(1)-C(2)-C(2)#1	-179.0(7)
Pd(1)-C(1)-N(1)-C(3)	-3.2(10)	C(3)-C(4)-C(5)-F(1)	177.3(5)
Pd(1)-N(2)-C(9)-C(10)	-177.7(6)	C(3)-C(4)-C(5)-C(6)	0.0(7)
Cl(1)-Pd(1)-C(1)-N(1)	-63.9(6)	C(4)-C(3)-C(8)-C(7)	-1.4(5)
Cl(1)-Pd(1)-C(1)-N(1)#1	116.1(6)	C(4)-C(5)-C(6)-C(7)	0.3(7)
C(1)-N(1)-C(2)-C(2)#1	-3.7(11)	C(5)-C(6)-C(7)-F(2)	-172.4(5)
C(1)-N(1)-C(3)-C(4)	137.7(6)	C(5)-C(6)-C(7)-C(8)	-1.1(6)
C(1)-N(1)-C(3)-C(8)	-40.6(9)	F(1)-C(5)-C(6)-C(7)	-177.0(5)
N(1)#1-C(1)-N(1)-C(2)	1.5(4)	C(6)-C(7)-C(8)-C(3)	1.6(5)
N(1)#1-C(1)-N(1)-C(3)	176.8(10)	F(2)-C(7)-C(8)-C(3)	171.1(5)
N(1)-C(3)-C(4)-C(5)	-177.7(5)	C(8)-C(3)-C(4)-C(5)	0.6(6)
N(1)-C(3)-C(8)-C(7)	176.8(5)	N(2)-C(9)-C(10)-C(11)	-5.0(14)
C(2)-N(1)-C(3)-C(4)	-47.1(9)	C(9)#1-N(2)-C(9)-C(10)	2.3(6)
C(2)-N(1)-C(3)-C(8)	134.6(7)	C(9)-C(10)-C(11)-C(10)#1	2.7(7)

Symmetry transformations to generate equivalent atoms: #1 -x+1, y, -z+1 #2 -x+1, -y+1, -z+1

The structure of 4c

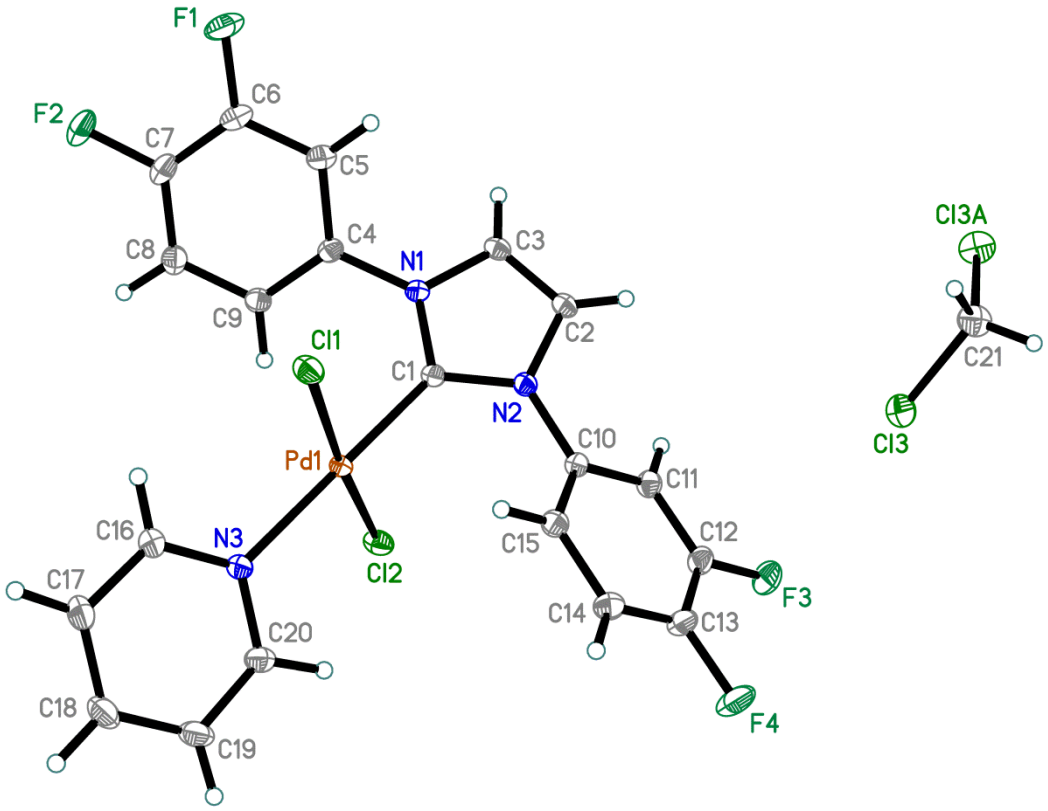

Figure S47. The molecular structure of **4c**·½CH_2Cl_2. Thermal ellipsoids are set to a 50% probability level.

Table S14. Selected bond distances for **4c** (Å).

Atoms	Distance	Atoms	Distance	Atoms	Distance
Pd(1)-Cl(1)	2.3155(3)	N(2)-C(1)	1.3563(14)	C(8)-C(9)	1.3935(16)
Pd(1)-Cl(2)	2.3178(3)	N(2)-C(2)	1.3962(14)	C(10)-C(11)	1.3963(16)
Pd(1)-N(3)	2.0872(10)	N(2)-C(10)	1.4283(14)	C(10)-C(15)	1.3917(16)
Pd(1)-C(1)	1.9558(11)	N(3)-C(16)	1.3481(16)	C(11)-C(12)	1.3807(16)
F(1)-C(6)	1.3392(14)	N(3)-C(20)	1.3441(15)	C(12)-C(13)	1.3814(18)
F(2)-C(7)	1.3497(14)	C(2)-C(3)	1.3459(16)	C(13)-C(14)	1.3814(18)
F(3)-C(12)	1.3436(14)	C(4)-C(5)	1.3918(16)	C(14)-C(15)	1.3962(16)
F(4)-C(13)	1.3439(14)	C(4)-C(9)	1.3919(16)	C(16)-C(17)	1.3852(18)
N(1)-C(1)	1.3582(14)	C(5)-C(6)	1.3806(17)	C(17)-C(18)	1.389(2)
N(1)-C(3)	1.3958(14)	C(6)-C(7)	1.3799(18)	C(18)-C(19)	1.387(2)
N(1)-C(4)	1.4277(14)	C(7)-C(8)	1.3849(17)		

Table S15. Selected bond angles for **4c** (°).

Atoms	Angle	Atoms	Angle
Cl(1)-Pd(1)-Cl(2)	175.042(10)	F(1)-C(6)-C(7)	119.41(11)
N(3)-Pd(1)-Cl(1)	91.57(3)	C(7)-C(6)-C(5)	120.89(11)
N(3)-Pd(1)-Cl(2)	93.38(3)	F(2)-C(7)-C(6)	118.79(11)
C(1)-Pd(1)-Cl(1)	87.49(3)	F(2)-C(7)-C(8)	120.32(12)
C(1)-Pd(1)-Cl(2)	87.57(3)	C(6)-C(7)-C(8)	120.89(11)
C(1)-Pd(1)-N(3)	178.63(4)	C(7)-C(8)-C(9)	119.00(11)
C(1)-N(1)-C(3)	110.72(9)	C(4)-C(9)-C(8)	119.58(10)
C(1)-N(1)-C(4)	125.07(9)	C(11)-C(10)-N(2)	117.57(10)
C(3)-N(1)-C(4)	124.13(9)	C(15)-C(10)-N(2)	121.36(10)
C(1)-N(2)-C(2)	110.67(9)	C(15)-C(10)-C(11)	121.06(10)
C(1)-N(2)-C(10)	126.10(9)	C(12)-C(11)-C(10)	118.46(11)
C(2)-N(2)-C(10)	123.21(9)	F(3)-C(12)-C(11)	119.55(11)
C(16)-N(3)-Pd(1)	121.76(8)	F(3)-C(12)-C(13)	119.54(11)
C(20)-N(3)-Pd(1)	119.77(8)	C(11)-C(12)-C(13)	120.90(11)
C(20)-N(3)-C(16)	118.34(10)	F(4)-C(13)-C(12)	118.62(11)
N(1)-C(1)-Pd(1)	127.18(8)	F(4)-C(13)-C(14)	120.55(12)
N(2)-C(1)-Pd(1)	127.81(8)	C(14)-C(13)-C(12)	120.83(11)
N(2)-C(1)-N(1)	104.98(9)	C(13)-C(14)-C(15)	119.28(11)
C(3)-C(2)-N(2)	106.88(10)	C(10)-C(15)-C(14)	119.44(11)
C(2)-C(3)-N(1)	106.74(9)	N(3)-C(16)-C(17)	122.32(12)
C(5)-C(4)-N(1)	117.84(10)	C(16)-C(17)-C(18)	119.04(13)
C(5)-C(4)-C(9)	121.14(10)	C(19)-C(18)-C(17)	118.75(12)
C(9)-C(4)-N(1)	121.02(10)	C(20)-C(19)-C(18)	119.03(12)
C(6)-C(5)-C(4)	118.43(11)	N(3)-C(20)-C(19)	122.51(12)
F(1)-C(6)-C(5)	119.68(12)		

Table S16. Torsion angles for **4c** (°).

Atoms	Angle	Atoms	Angle
Pd(1)-N(3)-C(16)-C(17)	-175.76(11)	C(4)-N(1)-C(1)-Pd(1)	1.12(16)
Pd(1)-N(3)-C(20)-C(19)	175.73(10)	C(4)-N(1)-C(1)-N(2)	-177.12(10)
F(1)-C(6)-C(7)-F(2)	-0.69(18)	C(4)-N(1)-C(3)-C(2)	176.60(10)
F(1)-C(6)-C(7)-C(8)	179.34(11)	C(4)-C(5)-C(6)-F(1)	178.87(11)
F(2)-C(7)-C(8)-C(9)	-178.28(11)	C(4)-C(5)-C(6)-C(7)	0.47(19)
F(3)-C(12)-C(13)-F(4)	-0.06(19)	C(5)-C(4)-C(9)-C(8)	-2.38(18)
F(3)-C(12)-C(13)-C(14)	179.33(12)	C(5)-C(6)-C(7)-F(2)	177.72(11)
F(4)-C(13)-C(14)-C(15)	179.76(12)	C(5)-C(6)-C(7)-C(8)	-2.26(19)
N(1)-C(4)-C(5)-C(6)	-177.97(11)	C(6)-C(7)-C(8)-C(9)	1.70(18)

N(1)-C(4)-C(9)-C(8)	177.43(10)	C(7)-C(8)-C(9)-C(4)	0.59(17)
N(2)-C(2)-C(3)-N(1)	0.72(13)	C(9)-C(4)-C(5)-C(6)	1.84(18)
N(2)-C(10)-C(11)-C(12)	179.39(11)	C(10)-N(2)-C(1)-Pd(1)	4.07(17)
N(2)-C(10)-C(15)-C(14)	179.41(11)	C(10)-N(2)-C(1)-N(1)	-177.70(10)
N(3)-C(16)-C(17)-C(18)	-0.2(2)	C(10)-N(2)-C(2)-C(3)	177.54(10)
C(1)-N(1)-C(3)-C(2)	-0.31(13)	C(10)-C(11)-C(12)-F(3)	-179.77(11)
C(1)-N(1)-C(4)-C(5)	139.93(12)	C(10)-C(11)-C(12)-C(13)	1.21(18)
C(1)-N(1)-C(4)-C(9)	-39.88(17)	C(11)-C(10)-C(15)-C(14)	-1.71(18)
C(1)-N(2)-C(2)-C(3)	-0.92(13)	C(11)-C(12)-C(13)-F(4)	178.95(12)
C(1)-N(2)-C(10)-C(11)	140.96(12)	C(11)-C(12)-C(13)-C(14)	-1.7(2)
C(1)-N(2)-C(10)-C(15)	-40.12(17)	C(12)-C(13)-C(14)-C(15)	0.4(2)
C(2)-N(2)-C(1)-Pd(1)	-177.52(8)	C(13)-C(14)-C(15)-C(10)	1.27(19)
C(2)-N(2)-C(1)-N(1)	0.71(12)	C(15)-C(10)-C(11)-C(12)	0.47(18)
C(2)-N(2)-C(10)-C(11)	-37.25(16)	C(16)-N(3)-C(20)-C(19)	-0.26(18)
C(2)-N(2)-C(10)-C(15)	141.67(12)	C(16)-C(17)-C(18)-C(19)	0.4(2)
C(3)-N(1)-C(1)-Pd(1)	178.00(8)	C(17)-C(18)-C(19)-C(20)	-0.5(2)
C(3)-N(1)-C(1)-N(2)	-0.25(12)	C(18)-C(19)-C(20)-N(3)	0.4(2)
C(3)-N(1)-C(4)-C(5)	-36.53(16)	C(20)-N(3)-C(16)-C(17)	0.16(19)
C(3)-N(1)-C(4)-C(9)	143.65(11)		

Table S17. Dihedral angles for **4c**, **4a2** and **4c**(°).

	Plane 1	Plane 2	Angle
4a1	N1, N2, C1, C2, C3	C4..C9	56.67(5)
	N1, N2, C1, C2, C3	C10..C15	63.02(5)
	N1, N2, C1, C2, C3	Pd1, Cl1, Cl2, C1, N3	76.66(4)
	Pd1, Cl1, Cl2, C1, N3	N3, C16..C20	29.28(5)
	Pd1, Cl1, Cl2, C1	Pd1, Cl1, Cl2, N3	8.09(5)
4a2	N1A, N2A, C1A, C2A, C3A	C4A..C9A	59.19(6)
	N1A, N2A, C1A, C2A, C3A	C10A..C15A	52.38(7)
	N1A, N2A, C1A, C2A, C3A	Pd1A, Cl1A, Cl2A, C1A, N3A	82.75(5)
	Pd1A, Cl1A, Cl2A, C1A, N3A	N3A, C16A..C20A	45.68(5)
	Pd1A, Cl1A, Cl2A, C1A	Pd1A, Cl1A, Cl2A, N3A	2.50(9)
	N1B, N2B, C1B, C2B, C3B	C4B..C9B	50.55(7)
	N1B, N2B, C1B, C2B, C3B	C10B..C15B	54.14(7)
	N1B, N2B, C1B, C2B, C3B	Pd1B, Cl1B, Cl2B, C1B, N3B	77.15(4)
	Pd1B, Cl1B, Cl2B, C1B, N3B	N3B, C16B..C20B	44.5 (3)
	Pd1B, Cl1B, Cl2B, C1B	Pd1B, Cl1B, Cl2B, N3B	7.33(2)
4c	N1, N2, C1, C2, C3	C4..C9	38.23(4)
	N1, N2, C1, C2, C3	C10..C15	38.30(4)
	N1, N2, C1, C2, C3	Pd1, Cl1, Cl2, C1, N3	70.87(3)
	Pd1, Cl1, Cl2, C1, N3	N3, C16..C20	41.41(3)
	Pd1, Cl1, Cl2, C1	Pd1, Cl1, Cl2, N3	1.27(6)

Table S18. Atom deviations from the $PdCl_2CN$ plane (Å).

Compound	Pd1	Cl1	Cl2	C1	N3
4a1	-0.0088(3)	-0.0807(3)	-0.0815(3)	0.0934(5)	0.0775(4)
4a2_A	-0.0212(4)	0.0372(4)	0.0370(4)	-0.0292(6)	-0.0238(5)
4a2_B	-0.0046(4)	0.0801(5)	0.0787(4)	-0.0827(7)	-0.0715(6)
4c	0.0040(3)	0.0115(3)	0.0113(3)	-0.0144(5)	-0.0124(4)

The core fragment $PdCl_2CN$ in **4a1** and in **4a2** (molecule *B*) is not entirely flat (Table S18): This fragment has a slightly bent conformation; $PdCl_2C$-$PdCl_2N$ folding angles are provided in Table S17.